

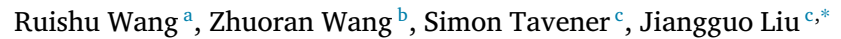
Contents lists available at ScienceDirect

Journal of Computational and Applied Mathematics

journal homepage: www.elsevier.com/locate/cam



Full weak Galerkin finite element discretizations for poroelasticity problems in the primal formulation



- ^a School of Mathematics, Jilin University, Changchun, Jilin 130012, China
- ^b Department of Mathematics, University of Kansas, Lawrence, KS 66049, USA
- ^c Department of Mathematics, Colorado State University, Fort Collins, CO 80523, USA

ARTICLE INFO

MSC:

65M12

65M60

74F10

74S05

Kevwords:

Arbogast-Correa spaces

Finite elements

Locking-free

Poroelasticity Quadrilateral meshes

Weak Galerkin

ABSTRACT

This paper develops novel finite element solvers for linear poroelasticity problems on quadrilateral meshes. These solvers are based on the primal formulations of linear elasticity and Darcy flow. Specifically, the fluid pressure and solid displacement are approximated by scalar-or vector-valued polynomials of degree $k \geq 0$ separately in element interiors and on edges. The discrete weak gradients of these shape functions are established in the broken (vector-or matrix-version) Arbogast–Correa spaces for approximations of the classical gradients in the variational forms. These weak Galerkin spatial discretizations are combined with the implicit Euler or Crank–Nicolson temporal discretizations to develop locking-free numerical solvers that have optimal order (k+1) convergence rates in pressure, velocity, displacement, stress, and dilation. Rigorous analysis is presented and illustrated by numerical experiments on popular test cases.

1. Introduction

In this paper, we consider the Biot's model for linear poroelasticity as shown below

$$\begin{cases}
-\nabla \cdot (2\mu \epsilon(\mathbf{u}) + \lambda(\nabla \cdot \mathbf{u})\mathbf{I}) + \alpha \nabla p = \mathbf{f}, & \text{in } \Omega \times (0, T], \\
\partial_t (\alpha \nabla \cdot \mathbf{u} + c_0 p) + \nabla \cdot (-\mathbf{K} \nabla p) = s, & \text{in } \Omega \times (0, T],
\end{cases}$$
(1)

where $\Omega \in \mathbb{R}^2$ is an open bounded and connected domain with Lipschitz continuous boundary $\partial \Omega$, \mathbf{u} is the solid displacement, $\varepsilon(\mathbf{u}) = \frac{1}{2} \left(\nabla \mathbf{u} + (\nabla \mathbf{u})^T \right)$ is the strain tensor, $\lambda = vE/\left((1-2v)(1+v) \right)$ and $\mu = E/\left(2(1+v) \right)$ are Lamé constants, $\sigma = 2\mu\varepsilon(\mathbf{u}) + \lambda(\nabla \cdot \mathbf{u})\mathbf{I}$ is the (effective) Cauchy stress (here \mathbf{I} is the identity matrix), \mathbf{f} is the body force, p is the fluid pressure, s is the fluid source (a sink is treated as a negative source), α (usually close to 1) is the Biot–Williams constant, $c_0 \ge 0$ is the coefficient for specific storage capacity, \mathbf{K} is the permeability tensor that has absorbed the fluid viscosity (for notational convenience) and is uniformly symmetric positive-definite. To close the PDE system, we consider the following boundary and initial conditions,

$$\begin{cases}
\mathbf{u}|_{\varGamma_{D}^{\mathcal{E}}} = \mathbf{u}_{D}, & ((\sigma - \alpha p \mathbf{I})\mathbf{n})|_{\varGamma_{N}^{\mathcal{E}}} = \mathbf{t}_{N}, & \text{on } \partial \Omega \times (0, T], \\
p|_{\varGamma_{D}^{\mathcal{D}}} = p_{D}, & -\mathbf{K} \nabla p \cdot \mathbf{n}|_{\varGamma_{N}^{\mathcal{D}}} = u_{N}, & \text{on } \partial \Omega \times (0, T], \\
\mathbf{u} = \mathbf{u}_{0}, & p = p_{0}, & \text{on } \Omega \times \{t = 0\}.
\end{cases}$$
(2)

E-mail addresses: wangrs_math@jlu.edu.cn (R. Wang), wangzr@ku.edu (Z. Wang), simon.tavener@colostate.edu (S. Tavener), liu@math.colostate.edu (J. Liu).

https://doi.org/10.1016/j.cam.2024.115754

Received 6 July 2023; Received in revised form 20 December 2023 Available online 9 January 2024 0377-0427/© 2024 Elsevier B.V. All rights reserved.



^{*} Corresponding author.

It is assumed that $\partial \Omega = \Gamma_D^D \cup \Gamma_N^D$ and $\partial \Omega = \Gamma_D^{\mathcal{E}} \cup \Gamma_N^{\mathcal{E}}$ are two non-overlapped partitions of the boundary $\partial \Omega$. Compatibility conditions $\mathbf{u}_0|_{\Gamma_D^{\mathcal{E}}} = \mathbf{u}_D$ and $p_0|_{\Gamma_D^{\mathcal{E}}} = p_D$ are also assumed.

The Biot's model for poroelasticity can be applied to many real-life problems, e.g., geosciences [1–4], biomechanics [5], tissue mechanics [6], and others [7]. Analytical solutions are unavailable for many cases, and hence accurate and robust numerical solvers will be the main focus.

Among the various types of numerical solvers for poroelasticity problems, finite element solvers based on the three-field formulations are the most popular, although the three fields could be different. Noticeable well designed such FE solvers can be found in [8–13].

A four-field formulation was adopted in [14] and then a solver based on mixed finite elements was developed. In a recent work [15], a four-field formulation was adopted and then conforming mixed FEs, e.g., Nédélec or BDM elements [16], were used for spatial discretizations. A five-field formulation of the Biot system was adopted in [17] for developing a mixed FE method that couples multipoint stress and multipoint flux, which was reduced to a cell-centered pressure–displacement system on simplicial and quadrilateral meshes.

Virtual element methods for poroelasticity were developed in [4,18,19]. With adoption of the enriched Galerkin (EG) methodology [20] for the approximation of solid displacement or fluid pressure, 2-field finite element solvers were developed in [3,21,22], local mass conservation and locking-free properties are satisfied.

The weak Galerkin (WG) methodology first introduced in [23] brings in new perspectives in development of finite element methods. WG FEMs have been developed for a wide range of differential equations [24,25], linear elasticity problems [26,27], the Maxwell equations [28], the Cahn–Hilliard equations [29], biharmonic problems [30], anisotropic diffusion problems [31], coupled Stokes–Darcy problems [32], parabolic problems [33]. Weak Galerkin FEMs for linear poroelasticity (Biot's consolidation model) can be found in [34–38].

Based on our previous work on any order WG FEMs for Darcy flow and linear elasticity [39,40], we develop in this paper two-field finite element solvers for linear poroelasticity on convex quadrilateral meshes, which are equally flexible as triangular meshes in accommodation of complicated domain geometry but could potentially use less unknowns and align better with physical features of the problems to be solved. In particular, we will use any order $k \ge 0$ polynomial WG shape functions in element interiors and on edges, scalar- or vector-valued. Their discrete weak gradients are constructed in the broken (vector- or matrix-version) Arbogast–Correa spaces [41], for which we have explicit local bases. The discrete weak gradients and discrete weak divergence (constructed as elementwise polynomials) are utilized to approximate the classical gradient and divergence in the variational formulations for Darcy flow and linear elasticity. Such full weak Galerkin spatial discretizations will be combined with the implicit Euler or Crank–Nicolson temporal discretization to develop two sets of new solvers for time-dependent poroelasticity problems. Rigorous analysis and numerical experiments on benchmarks will demonstrate that these new solvers are locking-free and have optimal order (k+1) accuracy displacement, stress, dilation, pressure, and velocity.

The rest of this paper is organized as follows. Section 2 presents WG finite element discretizations on convex quadrilateral meshes for Darcy flow and linear elasticity, respectively. Section 3 develops two sets of novel two-field finite element solvers (Algorithms I and II) for linear poroelasticity problems by combining the above full WG spatial discretizations with the implicit Euler or Crank–Nicolson temporal discretizations. Section 4 presents our main theoretical results (Theorems 1 and 2) on error estimates for these two sets of solvers, whereas details are postponed to Appendix. Numerical experiments are presented in Section 5 to illustrate the accuracy and locking-free property of these new solvers. Section 6 concludes the paper with remarks about on-going and future work.

2. Weak Galerkin finite element discretizations for Darcy flow and linear elasticity

2.1. Arbogast–Correa spaces $AC_k(k \ge 0)$ on quadrilaterals

For nonnegative integers $k \ge 0$, the AC_k spaces for vector-valued functions on quadrilaterals were developed in [41]. These spaces extend the traditional Raviart–Thomas spaces $RT_{[k]}$ on rectangles [16] to general convex quadrilaterals. Let E be a convex quadrilateral, the local Arbogast–Correa space is defined as

$$AC_k(E) = P_k(E)^2 + \widetilde{P}_k(E)\mathbf{x} + \mathbb{S}_k(E), \tag{3}$$

where $P_k(E)^2$ is the subspace of vector-valued polynomials with total degree $\leq k$, $\widetilde{P}_k(E)$ is the subspace of scalar-valued polynomials with degree = k, and $\mathbb{S}_k(E) = \mathcal{P}_E \hat{\mathbb{S}}_k$ is the subspace of rational functions obtained via the Piola transformation \mathcal{P}_E , where $\hat{\mathbb{S}}_k$ is defined on the reference element $\hat{E} = [0,1]^2$. The coordinates for the reference element are denoted as (\hat{x},\hat{y}) . Space $\hat{\mathbb{S}}_k$ can be generated as follows.

- For k=0, $\widehat{\mathbb{S}}_0 = \operatorname{Span}\{\operatorname{\mathbf{curl}}(\hat{x}\hat{y})\};$
- For $k \ge 1$,

$$\widehat{\mathbb{S}}_k = \text{Span}\{\text{curl}(\hat{x}^{k-1}\hat{y}(1-\hat{x}^2)), \text{ curl}(\hat{y}^{k-1}\hat{x}(1-\hat{y}^2))\}.$$

It should be noticed that in (3) the vector polynomials in $P_k(E)^2 + \widetilde{P}_k(E)\mathbf{x}$ are defined directly on the quadrilateral, whereas the shape functions (not necessarily polynomials) in $\mathbb{S}_k(E)$ are obtained via the Piola transformation.

It can be found in [41] that the degrees of freedom for $\mathbf{u} \in AC_k(E)$ are given by

$$\langle \mathbf{u} \cdot \mathbf{n}, v \rangle_{e} \qquad \forall v \in P_{k}(e), \forall e \subset \partial E,$$

$$\langle \mathbf{u}, \nabla w \rangle_{E} \qquad \forall w \in P_{k}(E),$$

$$\langle \mathbf{u}, \mathbf{v} \rangle_{F} \qquad \forall \mathbf{v} \in \mathbb{B}_{\nu}(E),$$

$$(4)$$

where **n** is the outward unit normal vector to ∂E and $\mathbb{B}_k(E)$ is a space of divergence-free bubble functions. Moreover, for any $\mathbf{u} \in AC_k(E)$, we have

$$\nabla \cdot \mathbf{u} \in P_k(E),$$

$$(\mathbf{u} \cdot \mathbf{n})|_e \in P_k(e), \quad \forall e \in \partial E.$$
(5)

Let \mathcal{E}_h be a shape-regular convex quadrilateral mesh for Ω . For any $E \in \mathcal{E}_h$, let h_E be the diameter of the circumscribed circle of E. Let $h = \max_{E \in \mathcal{E}_h} h_E$ be the mesh size. Let Γ_h be the set of all edges in \mathcal{E}_h . There are two types of global Arbogast–Correa spaces:

- The broken space: $\mathcal{AC}_k(\mathcal{E}_h) = \{\mathbf{v} \in L^2(\Omega)^2 : \mathbf{v}|_E \in \mathcal{AC}_k(E), \forall E \in \mathcal{E}_h\};$
- The H(div)-conforming subspace: $AC_k(\mathcal{E}_h) = \mathcal{AC}_k(\mathcal{E}_h) \cap H(\text{div}; \Omega)$.

Note that functions in $AC_k(\mathcal{E}_h)$ are continuous in the normal direction across edges.

We will also consider spaces of matrix-valued functions $AC_k(E)^2$, $AC_k(\mathcal{E}_h)^2$, or $AC_k(\mathcal{E}_h)^2$, whose row vectors are respectively in $AC_k(E)$, $AC_k(\mathcal{E}_h)$, or $AC_k(\mathcal{E}_h)$.

A linear poroelasticity problem couples Darcy flow for fluid pressure and linear elasticity for solid displacement. Next, we construct weak Galerkin finite elements for Darcy flow and linear elasticity, respectively.

2.2. $WG(P_k, P_k; AC_k)$ $(k \ge 0)$ finite element scheme for Darcy flow

For Darcy flow, we consider WG(P_k , P_k ; AC_k) finite elements. A discrete weak function $p_h = \{p^\circ, p^\partial\}$ has two parts: The interior part $p^\circ \in P_k(E^\circ)$ is defined in element interior E° for any $E \in \mathcal{E}_h$; The boundary part $p^\partial \in P_k(e)$ is defined for each edge $e \in \Gamma_h$. Note that p^∂ is not necessarily the trace of some p° . Denote by W_h the space of such weak functions p_h . Let W_h^0 be the subspace of W_h consisting of functions that vanish on Γ_D^D . For $p_h = \{p^\circ, p^\partial\} \in W_h$, we define its weak gradient $\nabla_w p_h \in \mathcal{AC}_k(\mathcal{E}_h)$ elementwise by

$$\int_{E} (\nabla_{w} p_{h}) \cdot \mathbf{w} = \int_{E^{\partial}} p^{\partial}(\mathbf{w} \cdot \mathbf{n}) - \int_{E^{\circ}} p^{\circ}(\nabla \cdot \mathbf{w}), \quad \forall \mathbf{w} \in AC_{k}(E), \ \forall E \in \mathcal{E}_{h}.$$

$$(6)$$

A weak Galerkin finite element scheme for the Darcy flow problem

$$\begin{cases}
\nabla \cdot (-\mathbf{K} \nabla p) \equiv \nabla \cdot \mathbf{u} = s, & \text{in } \Omega, \\
p|_{\Gamma_D^D} = p_D, & (\mathbf{u} \cdot \mathbf{n})|_{\Gamma_N^D} = u_N
\end{cases}$$
(7)

read as: Find $p_h \in W_h$ satisfying $p^{\partial}|_{\Gamma_D^D} = Q_h^{\partial}(p_D)$ and

$$\mathcal{A}_h^D(p_h,q_h) = \mathcal{F}_h^D(q_h), \quad \forall q_h = \{q^\circ,q^\partial\} \in W_h^0, \tag{8}$$

where

$$\mathcal{A}_{h}^{D}(p_{h},q_{h}) = \sum_{F \in \mathcal{E}_{h}} (\mathbf{K} \nabla_{w} p_{h}, \nabla_{w} q_{h})_{E}, \tag{9}$$

$$\mathcal{F}_{h}^{D}(q_{h}) = \sum_{E \in \mathcal{E}_{h}} (s, q^{\circ})_{E} - \sum_{e \in \Gamma_{N}^{D}} \langle u_{N}, q^{\partial} \rangle_{e}, \tag{10}$$

and Q_h^{∂} is the L^2 -projection operator onto space $P_k(e)$ for each edge $e \in \Gamma_h$.

The following functional defines a norm on space W_h^0 :

$$|||q_h||| = \left(\sum_{E \in \mathcal{E}_h} (\nabla_w q_h, \nabla_w q_h)_E\right)^{\frac{1}{2}}, \quad q_h \in W_h^0.$$

$$\tag{11}$$

The proof is very similar to that in [40] and hence omitted here.

2.3. $Wg(P_k^2, P_k^2; AC_k^2; P_k)$ $(k \ge 0)$ FE scheme for linear elasticity

For linear elasticity, we consider $\mathrm{WG}(P_k^2,P_k^2)$ -type vector-valued discrete weak functions. Such a function $\mathbf{v}_h = \{\mathbf{v}^\circ,\mathbf{v}^\partial\}$ has two parts: $\mathbf{v}^\circ \in P_k(E^\circ)^2$ is defined in the element interior E° for any $E \in \mathcal{E}_h$, whereas $\mathbf{v}^\partial \in P_k(e)^2$ is defined on each edge $e \in \Gamma_h$. Denote by \mathbf{V}_h the space of such weak functions and \mathbf{V}_h^0 the subspace of \mathbf{V}_h consisting of functions that vanish on $\Gamma_h^{\mathcal{E}}$.

For any $\mathbf{v}_h \in \mathbf{V}_h$, we establish its discrete weak gradient $\nabla_w \mathbf{v}_h \in \mathcal{AC}_k(\mathcal{E}_h)^2$ through integration by parts

$$\int_{E} (\nabla_{w} \mathbf{v}_{h}) : W = \int_{E^{\delta}} \mathbf{v}^{\delta} \cdot (W \mathbf{n}) - \int_{E^{\delta}} \mathbf{v}^{\circ} \cdot (\nabla \cdot W), \ \forall W \in AC_{k}(E)^{2}, \forall E \in \mathcal{E}_{h},$$

$$\tag{12}$$

where : is the standard colon product for matrices and \mathbf{n} is the outward unit normal vector on the boundary E^{∂} . We define the discrete weak strain as

$$\varepsilon_w(\mathbf{v}_h) = \frac{1}{2} \left(\nabla_w \mathbf{v}_h + (\nabla_w \mathbf{v}_h)^T \right).$$

Similarly, we establish its discrete weak divergence $\nabla_{uv} \cdot \mathbf{v} \in P_k(\mathcal{E}_h)$ by

$$\int_{E} (\nabla_{w} \cdot \mathbf{v}_{h}) w = \int_{E^{\vartheta}} \mathbf{v}^{\vartheta} \cdot (w\mathbf{n}) - \int_{E^{\circ}} \mathbf{v}^{\circ} \cdot (\nabla w), \quad \forall w \in P_{k}(E), \forall E \in \mathcal{E}_{h},$$
(13)

where $P_k(\mathcal{E}_h)$ is the space of piecewise polynomials with degree $\leq k$.

For the linear elasticity problem

$$\begin{cases}
-\nabla \cdot (2\mu\varepsilon(\mathbf{u}) + \lambda(\nabla \cdot \mathbf{u})\mathbf{I}) = \mathbf{f}, & \text{in } \Omega, \\
\mathbf{u}|_{\Gamma_D^{\mathcal{E}}} = \mathbf{u}_D, & (\sigma\mathbf{n})|_{\Gamma_N^{\mathcal{E}}} = \mathbf{t}_N,
\end{cases}$$
(14)

a weak Galerkin finite element scheme in the strain-div formulation reads as: Find $\mathbf{u}_h \in \mathbf{V}_h$ satisfying $\mathbf{u}^{\partial}|_{\Gamma_D^{\mathcal{E}}} = \mathbf{Q}_h^{\partial}(\mathbf{u}_D)$ and

$$\mathcal{A}_{h}^{\mathcal{E}}(\mathbf{u}_{h}, \mathbf{v}_{h}) = \mathcal{F}_{h}^{\mathcal{E}}(\mathbf{v}_{h}), \quad \forall \mathbf{v}_{h} \in \mathbf{V}_{h}^{0}, \tag{15}$$

where

$$\mathcal{A}_{h}^{\mathcal{E}}(\mathbf{u}_{h}, \mathbf{v}_{h}) = \sum_{E \in \mathcal{E}_{h}} 2\mu(\varepsilon_{w}(\mathbf{u}_{h}), \varepsilon_{w}(\mathbf{v}_{h}))_{E} + \lambda(\nabla_{w} \cdot \mathbf{u}_{h}, \nabla_{w} \cdot \mathbf{v}_{h})_{E}, \tag{16}$$

$$\mathcal{F}_{h}^{\mathcal{E}}(\mathbf{v}_{h}) = \sum_{E \in \mathcal{E}_{h}} (\mathbf{f}, \mathbf{v}^{\circ})_{E} + \sum_{e \in \Gamma^{\mathcal{E}}} \langle \mathbf{t}_{N}, \mathbf{v}^{\partial} \rangle_{e}, \tag{17}$$

and \mathbf{Q}_h^0 is the L^2 -projection operator onto space $P_k(e)^2$, $\forall e \in \Gamma_h$. Note that $\mathbf{t}_N = \sigma \mathbf{n}$ here is slightly different than that in the poroelasticity equation.

It has been shown in [40] that

$$\|\mathbf{v}_h\| := \left(\sum_{E \in \mathcal{C}} \|\nabla_w \mathbf{v}_h\|_E^2\right)^{\frac{1}{2}}, \quad \mathbf{v}_h \in \mathbf{V}_h^0$$

$$\tag{18}$$

is a norm on the space \mathbf{V}_{h}^{0} .

3. Two-field WG finite element solvers for linear poroelasticity problems

We now define some projection operators. Let

- Q_h° (or \mathbf{Q}_h°) be the L^2 -projection onto space $P_k(E)$ (or $P_k(E)^2$) for each element $E \in \mathcal{E}_h$;
- Q_h^{∂} (or Q_h^{∂}) be the L^2 -projection onto space $P_k(e)$ (or $P_k(e)^2$) on each edge $e \in \Gamma_h$;
- $Q_h = \{Q_h^{\circ}, Q_h^{\partial}\}\$ (or $\mathbf{Q}_h = \{\mathbf{Q}_h^{\circ}, \mathbf{Q}_h^{\partial}\}\$) be the L^2 -projection onto space $W_h(\text{or }\mathbf{V}_h)$;
- Q_h be the L^2 -projection into the broken Arbogast–Correa space $\mathcal{AC}_k(\mathcal{E}_h)$;
- \mathbb{Q}_h be the L^2 -projection into the broken Arbogast–Correa space $\mathcal{AC}_k(\mathcal{E}_h)^2$.

Properties in (5) of the AC spaces yield the following commuting identities, which are the most important properties of weak Galerkin finite elements. For any $\mathbf{u} \in H^1(\Omega)^2$ and any $p \in H^1(\Omega)$, there holds

$$\nabla_{uv}(\mathbf{Q}_{h}\mathbf{u}) = \mathbb{Q}_{h}(\nabla \mathbf{u}),
\nabla_{uv} \cdot (\mathbf{Q}_{h}\mathbf{u}) = \mathcal{Q}_{h}^{\circ}(\nabla \cdot \mathbf{u}),
\nabla_{uv}(\mathbf{Q}_{h}p) = \mathcal{Q}_{h}(\nabla p).$$
(19)

For space discretizations, we consider $WG(P_k, P_k; AC_k)$ FE scheme for fluid pressure and $WG(P_k^2, P_k^2; AC_k^2; P_k)$ FE scheme for solid displacement. The implicit Euler and the Crank–Nicolson temporal discretizations can be combined with any order discretization. But it will become clear that k = 0 matches well with the implicit Euler whereas k = 1 matches well with Crank–Nicolson.

Let N > 0 be an integer. Denote by $\Delta t = T/N$ the time step. Let $t_n = n\Delta t$ for n = 0, 1, ..., N. For a function **u** of space and time, denote $\mathbf{u}(\cdot, t_n)$ as $\mathbf{u}^{(n)}$.

3.1. Full WG discretizations combined with the implicit Euler

Algorithm I (Full WG FE discretizations combined with implicit Euler). The time-marching scheme starts with $\mathbf{u}_h^{(0)} = \mathbf{Q}_h \mathbf{u}_0$, $p_h^{(0)} = Q_h p_0$. Then for $1 \le n \le N$, seek $\mathbf{u}_h^{(n)} \in \mathbf{V}_h$ and $p_h^{(n)} \in W_h$ satisfying $\mathbf{u}^{(n),\partial}|_{\Gamma_D^{\mathcal{E}}} = \mathbf{Q}_h^{\partial} \mathbf{u}_D^{(n)}$ and $p_h^{(n),\partial}|_{\Gamma_D^D} = Q_h^{\partial} p_D^{(n)}$ such that for any $\mathbf{v}_h \in \mathbf{V}_h^0$ and any $q_h \in \mathbf{W}_h^0$,

$$\begin{cases}
A_{h}^{\mathcal{E}}(\mathbf{u}_{h}^{(n)}, \mathbf{v}_{h}) - B_{h}(\mathbf{v}_{h}, p_{h}^{(n)}) = \mathcal{F}_{h}^{\mathcal{E},(n)}(\mathbf{v}_{h}), \\
B_{h}\left(\frac{\mathbf{u}_{h}^{(n)} - \mathbf{u}_{h}^{(n-1)}}{\Delta t}, q_{h}\right) + C_{h}\left(\frac{p_{h}^{(n)} - p_{h}^{(n-1)}}{\Delta t}, q_{h}\right) \\
+ A_{h}^{D}(p_{h}^{(n)}, q_{h}) = \mathcal{F}_{h}^{D,(n)}(q_{h}),
\end{cases} (20)$$

This is equivalent to

$$\begin{cases}
\mathcal{A}_{h}^{\mathcal{E}}(\mathbf{u}_{h}^{(n)}, \mathbf{v}_{h}) - \mathcal{B}_{h}(\mathbf{v}_{h}, p_{h}^{(n)}) = \mathcal{F}_{h}^{\mathcal{E},(n)}(\mathbf{v}_{h}), \\
\mathcal{B}_{h}(\mathbf{u}_{h}^{(n)}, q_{h}) + \mathcal{C}_{h}(p_{h}^{(n)}, q_{h}) + \Delta t \mathcal{A}_{h}^{D}(p_{h}^{(n)}, q_{h}) = \mathcal{S}_{h}^{(n)}(q_{h}),
\end{cases} (21)$$

for all $\mathbf{v}_h \in \mathbf{V}_h^0$ and all $q_h \in \mathbf{W}_h^0$. The two new bilinear forms are

$$\begin{split} B_h(\mathbf{v}_h, q_h) &= \sum_{E \in \mathcal{E}_h} \alpha(\nabla_w \cdot \mathbf{v}_h, q^\circ)_E, \\ C_h(p_h, q) &= \sum_{E \in \mathcal{E}_r} c_0(p^\circ, q^\circ)_E. \end{split} \tag{22}$$

The linear forms are

with $\mathbf{t}_N = (\sigma - \alpha p \mathbf{I}) \mathbf{n}$.

$$\mathcal{F}_{h}^{\mathcal{E},(n)}(\mathbf{v}_{h}) = \sum_{E \in \mathcal{E}_{h}} (\mathbf{f}^{(n)}, \mathbf{v}^{\circ})_{E} + \sum_{e \in \Gamma_{N}^{\mathcal{E}}} \langle \mathbf{t}_{N}^{(n)}, \mathbf{v}^{\partial} \rangle_{e},$$

$$\mathcal{F}_{h}^{D,(n)}(q_{h}) = \sum_{E \in \mathcal{E}_{h}} (s^{(n)}, q^{\circ})_{E} - \sum_{e \in \Gamma_{N}^{D}} \langle u_{N}^{(n)}, q^{\partial} \rangle_{e},$$

$$\mathcal{S}_{h}^{(n)}(q_{h}) = \Delta t \mathcal{F}_{h}^{D,(n)}(q_{h}) + \mathcal{B}_{h}(\mathbf{u}_{h}^{(n-1)}, q_{h}) + \mathcal{C}_{h}(p_{h}^{(n-1)}, q_{h}),$$
(23)

3.2. Full WG discretizations combined with Crank-Nicolson

We consider space discretizations provided by $WG(P_k, P_k; AC_k)$ for fluid pressure and $WG(P_k^2, P_k^2; AC_k^2; P_k)$ for solid displacement for any $k \ge 1$. Of course, one can set k = 1 for simplicity.

Algorithm II (Full WG FE discretizations combined with Crank–Nicolson). The time-marching scheme starts with $\mathbf{u}_h^{(0)} = \mathbf{Q}_h \mathbf{u}_0$ and $p_h^{(0)} = Q_h p_0$. For $1 \le n \le N$, seek $\mathbf{u}_h^{(n)} \in \mathbf{V}_h$, $p_h^{(n)} \in W_h$ satisfying $\mathbf{u}^{(n),\partial}|_{\Gamma_D^{\mathcal{E}}} = \mathbf{Q}_h^{\partial} \mathbf{u}_D^{(n)}$ and $p_h^{(n),\partial}|_{\Gamma_D^{\mathcal{E}}} = Q_h^{\partial} p_D^{(n)}$ such that for any $\mathbf{v}_h \in \mathbf{V}_h^0$ and $q_h \in \mathbf{W}_h^0$, there holds

$$\mathcal{A}_{h}^{\mathcal{E}}\left(\frac{\mathbf{u}_{h}^{(n)} + \mathbf{u}_{h}^{(n-1)}}{2}, \mathbf{v}_{h}\right) - \mathcal{B}_{h}\left(\mathbf{v}_{h}, \frac{p_{h}^{(n)} + p_{h}^{(n-1)}}{2}\right) = \frac{\mathcal{F}_{h}^{\mathcal{E},(n)}(\mathbf{v}_{h}) + \mathcal{F}_{h}^{\mathcal{E},(n-1)}(\mathbf{v}_{h})}{2},
\mathcal{B}_{h}\left(\frac{\mathbf{u}_{h}^{(n)} - \mathbf{u}_{h}^{(n-1)}}{\Delta t}, q_{h}\right) + \mathcal{C}_{h}\left(\frac{p_{h}^{(n)} - p_{h}^{(n-1)}}{\Delta t}, q_{h}\right) + \mathcal{A}_{h}^{\mathcal{D}}\left(\frac{p_{h}^{(n)} + p_{h}^{(n-1)}}{2}, q_{h}\right)
= \frac{\mathcal{F}_{h}^{\mathcal{D},(n)}(q_{h}) + \mathcal{F}_{h}^{\mathcal{D},(n-1)}(q_{h})}{2}.$$
(24)

4. Analysis

We first address well-posedness of both Algorithm I and Algorithm II. For ease of presentation, we assume $\Gamma_D^D = \Gamma_D^{\mathcal{E}} = \partial \Omega$. For the bilinear form for linear elasticity, we adopt the grad-div formulation shown below for analysis.

$$\mathcal{A}_{h}^{\mathcal{E}}(\mathbf{u}_{h}, \mathbf{v}_{h}) = \sum_{E \in \mathcal{E}_{+}} \mu(\nabla_{w} \mathbf{u}_{h}, \nabla_{w} \mathbf{v}_{h})_{E} + (\lambda + \mu)(\nabla_{w} \cdot \mathbf{u}_{h}, \nabla_{w} \cdot \mathbf{v}_{h})_{E}. \tag{25}$$

This is not an unusual practice [42]. It is also known that the strain-div and grad-div formulations are equivalent when a Dirichlet condition is posed on the entire boundary.

Lemma 1. There exists a constant $\beta > 0$ such that

$$\inf_{q_h \in \mathcal{W}_h} \sup_{\mathbf{v}_h \in \mathcal{V}_h} \frac{\mathcal{B}_h(\mathbf{v}_h, q_h)}{\|\mathbf{v}_h\| \|q_h^\circ\|} \ge \beta. \tag{26}$$

Proof. It is known [43] that for any $q_h \in W_h$, there exists $\widetilde{\mathbf{w}} \in H^1(\Omega)^d$ so that

$$\frac{(\nabla \cdot \widetilde{\mathbf{w}}, \, q_h^{\circ})}{\|\nabla \widetilde{\mathbf{w}}\|} \ge C_1 \|q_h^{\circ}\|,$$

where $C_1 > 0$ is a constant independent of the choice of q_h . Let $\mathbf{w} = \mathbf{Q}_h \widetilde{\mathbf{w}} \in \mathbf{V}_h$. Using the first commuting identity in (19), we obtain

$$\|\!|\!|\!|\mathbf{w}|\!|\!|^2 = \sum_{E \in \mathcal{E}_h} \|\nabla_w \mathbf{w}\|_E^2 = \sum_{E \in \mathcal{E}_h} \|\nabla_w (\mathbf{Q}_h \widetilde{\mathbf{w}})\|_E^2 = \sum_{E \in \mathcal{E}_h} \|\mathbb{Q}_h (\nabla \widetilde{\mathbf{w}})\|_E^2 \leq \|\nabla \widetilde{\mathbf{w}}\|^2.$$

The second commuting identity in (19) implies

$$\sum_{E \in \mathcal{E}_h} (\nabla_w \cdot \mathbf{w}, \, q_h^{\circ})_E = \sum_{E \in \mathcal{E}_h} (\nabla_w \cdot (\mathbf{Q}_h \widetilde{\mathbf{w}}), \, q_h^{\circ})_E = \sum_{E \in \mathcal{E}_h} (Q_h^{\circ} \nabla \cdot \widetilde{\mathbf{w}}, \, q_h^{\circ})_E = \sum_{E \in \mathcal{E}_h} (\nabla \cdot \widetilde{\mathbf{w}}, \, q_h^{\circ})_E.$$

Therefore,

$$\sup_{\mathbf{v}_h \in \mathbf{V}_h} \frac{B_h(\mathbf{v}_h, q_h)}{\| \mathbf{v}_h \|} \geq \frac{\sum_{E \in \mathcal{E}_h} \alpha(\nabla_w \cdot \mathbf{w}, \ q_h^\circ)_E}{\| \mathbf{w} \|} \geq \alpha \frac{(\nabla \cdot \widetilde{\mathbf{w}}, \ q_h^\circ)}{\| \nabla \widetilde{\mathbf{w}} \|} \geq \beta \| q_h^\circ \|,$$

with $\beta = \alpha C_1$, as claimed. \square

Remark 1. From the definitions of the bilinear form $\mathcal{A}_h^{\mathcal{E}}(\cdot,\cdot)$ and norm $\|\cdot\|$, we know that this bilinear form is coercive, i.e.,

$$\mathcal{A}_h^{\mathcal{E}}(\mathbf{v}_h,\mathbf{v}_h) = \sum_{E \in \mathcal{E}_h} \mu(\nabla_w \mathbf{v}_h,\nabla_w \mathbf{v}_h)_E + (\lambda + \mu)(\nabla_w \cdot \mathbf{v}_h,\nabla_w \cdot \mathbf{v}_h)_E \geq \mu \|\|\mathbf{v}_h\|\|^2.$$

As for the bilinear form $C_h(\cdot,\cdot) + \Delta t \, \mathcal{A}_h^D(\cdot,\cdot)$, we cannot claim coercivity, since parameter $c_0 = 0$ is possible and Δt approaches zero. It is reasonable to assume the permeability tensor has a positive lower bound, that is,

$$\int_{E} \xi^{T} \mathbf{K} \xi d\mathbf{x} \ge m_{\mathbf{K}} \int_{E} \xi \cdot \xi d\mathbf{x} > 0, \quad \forall \xi \in AC_{k}(E), \ \forall E \in \mathcal{E}_{h},$$

$$(27)$$

with the constant $m_K > 0$. It is known from [37] that there exists a constant C > 0 such that

$$\|q_h^o\| \le C\|\nabla_w q_h\|, \quad \forall q_h \in W_h^0. \tag{28}$$

Therefore, the bilinear form $C_h(\cdot,\cdot) + \Delta t A_h^D(\cdot,\cdot)$ is nonnegative, in other words,

$$\begin{split} C_h(q_h,q_h) + \Delta t \, \mathcal{A}_h^D(q_h,q_h) &= \sum_{E \in \mathcal{E}_h} c_0(q_h^\circ,q_h^\circ)_E + \Delta t \sum_{E \in \mathcal{E}_h} (\mathbf{K} \nabla_w q_h, \nabla_w q_h)_E \\ &\geq (c_0 + \Delta t \, m_\mathbf{K} C^{-2}) \|q_h^\circ\|^2 \geq 0. \end{split}$$

Note also that the skeleton part q_h^{∂} of q_h is not included in the inf-sup condition (26), since it is not used in the bilinear form $\mathcal{B}_h(\mathbf{v}_h,q_h)$.

Lemma 2. For each time step $n \in \{1, ..., N\}$, the solution $(\mathbf{u}_h^{(n)}, p_h^{(n)}) \in \mathbf{V}_h \times W_h$ of Algorithm I or II exists and is unique.

Proof. It is clear that at each time step n, Algorithm I and II can be rewritten as: Finding $\mathbf{u}_h^{(n)} \in \mathbf{V}_h$ and $p_h^{(n)} \in \mathbf{W}_h$ such that

$$\begin{cases} \mathcal{A}_{h}^{\mathcal{E}}(\mathbf{u}_{h}^{(n)}, \mathbf{v}_{h}) - \mathcal{B}_{h}(\mathbf{v}_{h}, p_{h}^{(n)}) = RHS_{1}, \\ \mathcal{B}_{h}(\mathbf{u}_{h}^{(n)}, q_{h}) + \mathcal{C}_{h}(p_{h}^{(n)}, q_{h}) + \Delta t \, \mathcal{A}_{h}^{D}(p_{h}^{(n)}, q_{h}) = RHS_{2}, \end{cases}$$
(29)

for any $\mathbf{v}_h \in \mathbf{V}_h^0$ and $q_h \in W_h^0$. The right-hand side terms RHS₁ and RHS₂ can be readily identified from Algorithm I or Algorithm II. Assume RHS₁ = 0 or RHS₂ = 0. Let $\mathbf{v}_h = \mathbf{u}_h^{(n)}$ and $q_h = p_h^{(n)}$. Summing up the two equations in (29) yields

$$\mathcal{A}_{h}^{\mathcal{E}}(\mathbf{u}_{h}^{(n)},\mathbf{u}_{h}^{(n)}) + C_{h}(p_{h}^{(n)},p_{h}^{(n)}) + \Delta t \, \mathcal{A}_{h}^{\mathcal{D}}(p_{h}^{(n)},p_{h}^{(n)}) = 0.$$

The definitions of the bilinear forms $\mathcal{A}_{h}^{\mathcal{E}}(\cdot,\cdot)$ and $\mathcal{C}_{h}(\cdot,\cdot) + \Delta t \,\mathcal{A}_{h}^{\mathcal{D}}(\cdot,\cdot)$ imply that

$$\|\mathbf{u}_{h}^{(n)}\| = 0, \quad \|p_{h}^{(n)}\| = 0.$$

for which we have used the assumption (27) about the permeability tensor. Since Algorithm (29) is a finite-dimensional linear problem, the existence of the solution can be derived from the uniqueness. \Box

For analysis, we need two interpolation operators defined as $\pi_h: H(\operatorname{div};\Omega) \to AC_k(\mathcal{E}_h)$ and $\Pi_h: H(\operatorname{div};\Omega)^2 \to AC_k(\mathcal{E}_h)^2$. They satisfy the following properties:

(i). For any $\mathbf{v} \in H(\text{div}; \Omega)$ and $\tau \in H(\text{div}; \Omega)^2$,

$$(\nabla \cdot \mathbf{v}, q)_E = (\nabla \cdot (\pi_h \mathbf{v}), q)_E, \quad \forall q \in P_k(E), \forall E \in \mathcal{E}_h, (\nabla \cdot \tau, \mathbf{w})_E = (\nabla \cdot (\Pi_h \tau), \mathbf{w})_E, \quad \forall \mathbf{w} \in P_k(E)^2, \forall E \in \mathcal{E}_h.$$

$$(30)$$

(ii). For any $\mathbf{v} \in H^{k+1}(\Omega)^2$, $\tau \in H^{k+1}(\Omega)^{2\times 2}$, and $k \ge 0$,

$$\|\mathbf{v} - \pi_h \mathbf{v}\| \lesssim h^{k+1} \|\mathbf{v}\|_{k+1}, \|\tau - \Pi_h \tau\| \lesssim h^{k+1} \|\tau\|_{k+1}.$$
(31)

(iii). When $\Gamma_D^D = \Gamma_D^{\mathcal{E}} = \partial \Omega$, the above properties combined with the definitions of discrete weak gradients and the fact that $AC_k(\mathcal{E}_h) \subset H(\operatorname{div};\Omega)$ imply that

$$\sum_{E \in \mathcal{E}_h} (-\nabla \cdot \mathbf{v}, q_h^{\circ})_E = \sum_{E \in \mathcal{E}_h} (\pi_h \mathbf{v}, \nabla_w q_h)_E, \quad \forall q_h = \{q_h^{\circ}, q_h^{\partial}\} \in W_h^0, \tag{32}$$

$$\sum_{E \in \mathcal{E}_h} (-\nabla \cdot \tau, \mathbf{v}_h^{\circ})_E = \sum_{E \in \mathcal{E}_h} (\Pi_h \tau, \nabla_w \mathbf{v}_h)_E, \quad \forall \mathbf{v}_h = \{\mathbf{v}_h^{\circ}, \mathbf{v}_h^{\partial}\} \in \mathbf{V}_h^0.$$
(33)

Lemma 3. For any $\mathbf{u} \in H^1(\Omega)^2$ and $p \in H^1(\Omega)$, there hold

$$\mathcal{A}_{h}^{\mathcal{E}}(\mathbf{Q}_{h}\mathbf{u},\mathbf{v}_{h}) = \sum_{E \in \mathcal{E}_{h}} (\mu \nabla_{w}(\mathbf{Q}_{h}\mathbf{u}) + (\lambda + \mu)(\nabla_{w} \cdot \mathbf{Q}_{h}\mathbf{u})\mathbf{I}, \nabla_{w}\mathbf{v}_{h})_{E},$$

$$\mathcal{B}_{h}(\mathbf{v}_{h}, Q_{h}p) = \sum_{E \in \mathcal{E}_{h}} \alpha(\nabla_{w}\mathbf{v}_{h}, (Q_{h}^{\circ}p)\mathbf{I})_{E},$$

$$\mathcal{B}_{h}(\mathbf{Q}_{h}\mathbf{u}, q_{h}) = \sum_{E \in \mathcal{E}_{h}} \alpha(\nabla \cdot \mathbf{u}, q^{\circ})_{E},$$

$$\mathcal{C}_{h}(Q_{h}p, q_{h}) = \sum_{E \in \mathcal{E}_{h}} c_{0}(p, q^{\circ})_{E},$$

$$\mathcal{A}_{h}^{D}(Q_{h}p, q_{h}) = \sum_{E \in \mathcal{E}_{h}} (\mathbf{K}\nabla_{w}(Q_{h}p), \nabla_{w}q_{h})_{E},$$
(34)

for any $\mathbf{v}_h \in \mathbf{V}_h^0$ and $q_h \in W_h^0$.

Proof. For any function $w \in P_k(\mathcal{E}_h)$, since $w\mathbf{I} \in \mathcal{AC}_k(\mathcal{E}_h)^2$, we have

$$\sum_{E \in \mathcal{E}_h} (\nabla_w \cdot \mathbf{v}_h, w)_E = \sum_{E \in \mathcal{E}_h} (\nabla_w \mathbf{v}_h, w \mathbf{I})_E, \ \, \forall \mathbf{v}_h \in \mathbf{V}_h^0.$$

Taking $w = \nabla_w \cdot \mathbf{Q}_h \mathbf{u}$ and $w = Q_h^{\circ} p$, respectively, we obtain

$$\sum_{E \in \mathcal{E}_h} (\nabla_w \cdot \mathbf{Q}_h \mathbf{u}, \nabla_w \cdot \mathbf{v}_h)_E = \sum_{E \in \mathcal{E}_h} ((\nabla_w \cdot \mathbf{Q}_h \mathbf{u}) \mathbf{I}, \nabla_w \mathbf{v}_h)_E,
\sum_{E \in \mathcal{E}_h} (\nabla_w \cdot \mathbf{v}_h, Q_h^{\circ} p)_E = \sum_{E \in \mathcal{E}_h} (\nabla_w \mathbf{v}_h, (Q_h^{\circ} p) \mathbf{I})_E.$$
(35)

Applying the commuting identity (11) and the definitions of the projection operators, we reach the conclusion of this lemma. \Box

Lemma 4. Let $\mathbf{u} \in H^2(\Omega)^2$ and $p \in H^2(\Omega)$ be the solutions of poroelasticity problem (1). Then we have, for any $\mathbf{v}_h \in \mathbf{V}_h^0$ and $q_h \in W_h^0$,

$$\begin{split} &\sum_{E \in \mathcal{E}_h} (\mathbf{f}, \mathbf{v}_h^{\circ})_E = \sum_{E \in \mathcal{E}_h} (\mu \Pi_h(\nabla \mathbf{u}) + (\lambda + \mu) \Pi_h((\nabla \cdot \mathbf{u})\mathbf{I}) - \alpha \Pi_h(p\mathbf{I}), \nabla_w \mathbf{v}_h)_E, \\ &\sum_{E \in \mathcal{E}_h} (s, q_h^{\circ})_E = \sum_{E \in \mathcal{E}_h} (\partial_t (\alpha \nabla \cdot \mathbf{u} + c_0 p), q_h^{\circ})_E + \sum_{E \in \mathcal{E}_h} (\pi_h(\mathbf{K} \nabla p), \nabla_w q_h)_E, \end{split} \tag{36}$$

Proof. It is clear that

$$-\nabla \cdot (2\mu\varepsilon(\mathbf{u}) + \lambda(\nabla \cdot \mathbf{u})\mathbf{I}) + \alpha\nabla p = -\nabla \cdot (\mu\nabla\mathbf{u} + (\lambda + \mu)(\nabla \cdot \mathbf{u})\mathbf{I} - \alpha p\mathbf{I}).$$

One tests the PDE by the interior parts \mathbf{v}° , q° of discrete weak functions $\mathbf{v}_h \in \mathbf{V}_h^0$, $q_h \in W_h^0$. Applying (32) (33) leads to the desired conclusion.

4.1. Analysis for Algorithm I

Lemma 5. Let $\mathbf{u} \in H^2(\Omega)^2$, $p \in H^2(\Omega)$ be the solutions of Problem (1). Let $\mathbf{u}_h \in \mathbf{V}_h$, $p_h \in W_h$ be the numerical solutions of Algorithm I. Let $\xi_h = \mathbf{Q}_h \mathbf{u} - \mathbf{u}_h \in \mathbf{V}_h^0$, $\zeta_h = Q_h p - p_h \in W_h^0$. Then the error equations are

$$\mathcal{A}_{h}^{\mathcal{E}}(\xi_{h}^{(n)}, \mathbf{v}_{h}) - \mathcal{B}_{h}(\mathbf{v}_{h}, \zeta_{h}^{(n)}) = \sum_{E \in \mathcal{E}_{h}} (\phi(\mathbf{u}^{(n)}) + \psi(p^{(n)}), \nabla_{w} \mathbf{v}_{h})_{E},$$

$$\mathcal{B}_{h}\left(\frac{\xi_{h}^{(n)} - \xi_{h}^{(n-1)}}{\Delta t}, q_{h}\right) + C_{h}\left(\frac{\zeta_{h}^{(n)} - \zeta_{h}^{(n-1)}}{\Delta t}, q_{h}\right) + \mathcal{A}_{h}^{D}(\zeta_{h}^{(n)}, q_{h})$$

$$= \sum_{E \in \mathcal{E}_{h}} (\phi(p^{(n)}), \nabla_{w} q_{h})_{E} + \sum_{E \in \mathcal{E}_{h}} (\alpha \nabla \cdot \mathbf{R}(\mathbf{u}, t_{n}) + c_{0} \mathbf{R}(p, t_{n}), q^{\circ})_{E},$$
(37)

where the remainders are

$$\begin{cases} \phi(\mathbf{u}^{(n)}) = \mu(\nabla_{w}(\mathbf{Q}_{h}\mathbf{u}^{(n)}) - \Pi_{h}(\nabla\mathbf{u}^{(n)})) \\ + (\lambda + \mu)(\nabla_{w} \cdot (\mathbf{Q}_{h}\mathbf{u}^{(n)})\mathbf{I} - \Pi_{h}((\nabla \cdot \mathbf{u}^{(n)})\mathbf{I})), \\ \psi(p^{(n)}) = \alpha(\Pi_{h}(p^{(n)}\mathbf{I}) - Q_{h}^{\circ}(p^{(n)}\mathbf{I})), \\ \varphi(p^{(n)}) = \mathbf{K}\nabla_{w}(Q_{h}p^{(n)}) - \pi_{h}(\mathbf{K}\nabla p^{(n)}), \end{cases}$$
(38)

and

$$\left\{ \begin{array}{l} \mathbf{R}(\mathbf{u},t_n) = \frac{1}{\Delta t} \int_{t_{n-1}}^{t_n} (\tau - t_{n-1}) \partial_{tt} \mathbf{u}(\tau) d\tau, \\ \\ \mathbf{R}(p,t_n) = \frac{1}{\Delta t} \int_{t_{n-1}}^{t_n} (\tau - t_{n-1}) \partial_{tt} p(\tau) d\tau. \end{array} \right.$$

Proof. Take $t = t_n$ in Lemmas 3 and 4. Applying the facts that

$$\frac{\mathbf{u}^{(n)} - \mathbf{u}^{(n-1)}}{\Delta t} - \partial_t \mathbf{u}^{(n)} = \frac{1}{\Delta t} \int_{t_{n-1}}^{t_n} (\tau - t_{n-1}) \partial_{tt} \mathbf{u}(\tau) d\tau =: \mathbf{R}(\mathbf{u}, t_n),$$

$$\frac{p^{(n)} - p^{(n-1)}}{\Delta t} - \partial_t p^{(n)} = \frac{1}{\Delta t} \int_{t_{n-1}}^{t_n} (\tau - t_{n-1}) \partial_{tt} p(\tau) d\tau =: \mathbf{R}(p, t_n),$$
(39)

we reach the conclusion of this lemma. \Box

Theorem 1. Let (\mathbf{u}, p) be the exact solutions of poroelasticity problem (1). Let $\mathbf{u}_h \in \mathbf{V}_h$ and $p_h \in \mathbf{W}_h$ be the numerical solutions of (21) by Algorithm I. Let $\xi_h = \mathbf{Q}_h \mathbf{u} - \mathbf{u}_h \in \mathbf{V}_h^0$ and $\zeta_h = Q_h p - p_h \in \mathbf{W}_h^0$. Then under the following assumptions about regularity of the exact solutions

$$\begin{aligned} &\mathbf{u} \in [L^{\infty}(0,T;H^{k+2}(\Omega))]^{2}, \quad p \in L^{\infty}(0,T;H^{k+2}(\Omega)), \\ &\partial_{t}\mathbf{u} \in [L^{\infty}(0,T;H^{k+2}(\Omega))]^{2}, \quad \partial_{t}p \in L^{\infty}(0,T;H^{k+1}(\Omega)), \\ &\partial_{t}\mathbf{u} \in [L^{2}(0,T;H^{k+2}(\Omega))]^{2}, \quad \partial_{tt}p \in L^{2}(0,T;H^{k+1}(\Omega)), \end{aligned} \tag{40}$$

there holds an error estimate

$$\max_{1 \le n \le N} \left\{ \|\nabla_{w} \xi_{h}^{(n)}\|^{2} + \lambda \|\nabla_{w} \cdot \xi_{h}^{(n)}\|^{2} + \|\xi_{h}^{\circ,(n)}\|^{2} \right\} \\
+ \sum_{1}^{N} \Delta t \|\nabla_{w} \xi_{h}^{(n)}\|^{2} \le \mathcal{O}\left(h^{2(k+1)} + \Delta t^{2}\right). \tag{41}$$

Note that after taking square roots, the errors of displacement, dilation, pressure, and velocity, measured in the L_2 -norm, are actually of (k+1)st order.

Proof. See Appendix. □

4.2. Analysis for Algorithm II

For convenience, we denote $\frac{\mathbf{u}^{(n)}+\mathbf{u}^{(n-1)}}{2}$ by $\bar{\mathbf{u}}^{n-\frac{1}{2}}$ for a vector-valued function \mathbf{u} . For ease of presentation, we focus on the case k=1.

Lemma 6. Assume $\mathbf{u} \in H^2(\Omega)^2$ and $p \in H^2(\Omega)$ be the exact solutions of poroelasticity problem (1). Let $\mathbf{u}_h \in \mathbf{V}_h$ and $p_h \in W_h$ be the numerical solutions of (21) by Algorithm II. Let $\xi_h = \mathbf{Q}_h \mathbf{u} - \mathbf{u}_h \in \mathbf{V}_h^0$ and $\zeta_h = Q_h p - p_h \in W_h^0$. We can establish the following error equations.

$$\mathcal{A}_{h}^{\mathcal{E}}\left(\bar{\xi}_{h}^{n-\frac{1}{2}}, \mathbf{v}_{h}\right) - \mathcal{B}_{h}\left(\mathbf{v}_{h}, \bar{\zeta}_{h}^{n-\frac{1}{2}}\right) = \sum_{E \in \mathcal{E}_{h}} (\phi(\bar{\mathbf{u}}^{n-\frac{1}{2}}) + \psi(\bar{p}^{n-\frac{1}{2}}), \nabla_{w}\mathbf{v}_{h})_{E},$$

$$\mathcal{B}_{h}\left(\frac{\xi_{h}^{(n)} - \xi_{h}^{(n-1)}}{\Delta t}, q_{h}\right) + C_{h}\left(\frac{\zeta_{h}^{(n)} - \zeta_{h}^{(n-1)}}{\Delta t}, q_{h}\right) + \mathcal{A}_{h}^{D}\left(\bar{\zeta}_{h}^{n-\frac{1}{2}}, q_{h}\right)$$

$$= (\varphi(\bar{p}^{(n-\frac{1}{2})}), \nabla_{w}q_{h}) + \sum_{E \in \mathcal{E}_{h}} (\alpha\nabla \cdot \widetilde{\mathbf{R}}(\mathbf{u}, t_{h}) + c_{0}\widetilde{\mathbf{R}}(p, t_{h}), q^{\circ})_{E},$$
(42)

where

$$\left\{ \begin{array}{l} \widetilde{\mathbf{R}}(\mathbf{u},t_n) = \frac{\mathbf{u}^{(n)} - \mathbf{u}^{(n-1)}}{\Delta t} - \partial_t \bar{\mathbf{u}}^{n-\frac{1}{2}}, \\ \widetilde{\mathbf{R}}(p,t_n) = \frac{p^{(n)} - p^{(n-1)}}{\Delta t} - \partial_t \bar{p}^{n-\frac{1}{2}}. \end{array} \right.$$

Proof. This can be obtained in a straightforward way by taking $t = t_n$ and $t = t_{n-1}$ in Lemmas 3 and 4.

Theorem 2. Assume the exact solutions (\mathbf{u}, p) of poroelasticity problem (1) satisfy the regularity assumptions (40). Let $\mathbf{u}_h \in \mathbf{V}_h$ and $p_h \in W_h$ be the numerical solutions of (21) by Algorithm II. Let $\xi_h = \mathbf{Q}_h \mathbf{u} - \mathbf{u}_h \in \mathbf{V}_h^0$ and $\zeta_h = Q_h p - p_h \in W_h^0$. The following error estimate holds.

$$\max_{1 \le n \le N} \left\{ \|\nabla_{w} \xi_{h}^{(n)}\|^{2} + \lambda \|\nabla_{w} \cdot \xi_{h}^{(n)}\|^{2} + \|\xi_{h}^{\circ,(n)}\|^{2} \right\} + \sum_{n=1}^{N} \Delta t \|\nabla_{w} \xi_{h}^{n-\frac{1}{2}}\|^{2} \le \mathcal{O}(h^{4} + \Delta t^{4}).$$
(43)

Obviously, after taking square roots, the errors for displacement, dilation, pressure, and velocity, measured in the L_2 -norms, are actually of 2nd order.

Proof. See Appendix. □

Theorem 3. For two-dimensional problems (d = 2) and k = 0, under the regularity assumption [44] for the exact solution $\mathbf{u} \in H^2(\Omega)^d$ that

$$\mu \|\mathbf{u}\|_2 + \lambda \|\nabla \cdot \mathbf{u}\|_1 \le C \|\mathbf{f}\|_0 \tag{44}$$

with C>0 being a constant independent of \mathbf{u},\mathbf{f} , the numerical solution of Algorithm I is locking-free in the sense that

$$\max_{1 \le n \le N} \| \mathbf{Q}_h \mathbf{u}^{(n)} - \mathbf{u}_h^{(n)} \| \le C(h + \Delta t),$$

$$\max_{1 \le n \le N} \| \mathbf{u}^{(n)} - \mathbf{u}_h^{(n)} \| \le C(h + \Delta t),$$
(45)

where the positive constant C is independent of λ and h.

For $k \ge 1$, we need a stronger regularity assumption [45] in a similar form

$$\mu \|\mathbf{u}\|_{k+2} + \lambda \|\nabla \cdot \mathbf{u}\|_{k+1} \le C \|\mathbf{f}\|_{k} \tag{46}$$

with C>0 being a constant independent of \mathbf{u},\mathbf{f} . Accordingly, the numerical solutions of Algorithms I and II are locking-free, that is,

$$\max_{1 \le n \le N} \| \mathbf{Q}_h \mathbf{u}^{(n)} - \mathbf{u}_h^{(n)} \| \le C \left(h^{k+1} + \Delta t \right),$$

$$\max_{1 \le n \le N} \| \mathbf{u}^{(n)} - \mathbf{u}_h^{(n)} \| \le C \left(h^{k+1} + \Delta t \right),$$

$$(47)$$

where C > 0 is a constant independent of λ and h.

Proof. See Appendix. □

5. Numerical experiments

This section presents numerical experiments on our 2-field finite element solvers that utilize the implicit Euler or Crank–Nicolson for temporal discretization, the weak Galerkin $(P_k, P_k; AC_k)(k \ge 0)$ elements for Darcy flow, and the weak Galerkin $(P_k^2, P_k^2; AC_k^2; P_k)$ elements for linear elasticity.

Example 1 (*Smooth Solutions*). This example is adopted from [46] with slight modifications. Here $\Omega = (0, 1)^2$, T = 1, K = I, $C_0 = 0$, and $\alpha = 1$. The analytical solutions are known as

$$\mathbf{u} = t \begin{bmatrix} \sin(2\pi y)(-1 + \cos(2\pi x)) + \frac{1}{\mu + \lambda}\sin(\pi x)\sin(\pi y) \\ \sin(2\pi x)(1 - \cos(2\pi y)) + \frac{1}{\mu + \lambda}\sin(\pi x)\sin(\pi y) \end{bmatrix}$$

and

$$p = -t\sin(\pi x)\sin(\pi y).$$

Dirichlet boundary conditions are posed for the whole boundary using the values of the exact solutions.

To effectively demonstrate the locking-free property of our solvers, we choose the Poisson ratio as $\nu=0.49999$, which is close to 0.5. Thus $\lambda=16666$ and $\mu=0.33334$. Notably, the full WG solvers are specifically tested on the trapezoidal meshes used [47]. The numerical results shown in Tables 1 and 2 exhibit optimal order convergence in the errors of displacement, dilation, stress, pressure, and velocity. In Table 3, the results obtained from WG(P_1^2 , P_1^2 ; AC_1^2 ; P_1) + WG(P_1 , P_1 ; AC_1) and Crank–Nicolson demonstrate clearly second-order convergence of all errors. It is worth noting that our solvers are effective on rectangular meshes as well but the results are omitted due to page limitation.

Table 1 Example 1: Optimal convergence rates of the 2-field solver $WG(P_0^2, P_0^2; AC_0^2; P_0) + WG(P_0, P_0; AC_0)$ on trapezoidal meshes (slant parameter 0.35, see [47]) combined with implicit Euler and $\Delta t = h$.

h	$\ \mathbf{u} - \mathbf{u}_h^{\circ}\ _{l^2(L^2)}$	Rate	$ p-p_h^{\circ} _{l^2(L^2)}$	Rate	$\ \mathbf{q}-\mathbf{q}_h\ _{l^2(L^2)}$	Rate	$\ \nabla \cdot \mathbf{u} - \nabla \cdot \mathbf{u}_h\ _{l^2(L^2)}$	Rate	$\ \sigma-\sigma_h\ _{l^2(L^2)}$	Rate
2^{-3}	2.1355e-1	_	5.2852e-2	-	1.7438e-1	-	1.5202e-5	-	7.4037e-1	-
2^{-4}	1.0181e-1	1.06	2.5375e-2	1.05	8.4363e-2	1.04	7.2055e-6	1.07	3.5543e-1	1.05
2^{-5}	4.9694e-2	1.03	1.2413e-2	1.03	4.1528e-2	1.02	3.4937e-6	1.04	1.7384e-1	1.03
2^{-6}	2.4553e-2	1.01	6.1369e-3	1.01	2.0603e-2	1.01	1.7201e-6	1.02	8.5921e-2	1.01
2^{-7}	1.2204e-2	1.00	3.0508e-3	1.00	1.0261e-2	1.00	8.5373e-7	1.01	4.2708e-2	1.00

Table 2 Example 1: Results of the 2-field solver $WG(P_1^2, P_1^2; AC_1^2; P_1) + WG(P_1, P_1; AC_1)$ on trapezoidal meshes (slant parameter 0.35, see [47]) combined with implicit Euler and $\Delta t = h^2$.

h	$\ \mathbf{u} - \mathbf{u}_h^{\circ}\ _{l^2(L^2)}$	Rate	$ p-p_h^{\circ} _{l^2(L^2)}$	Rate	$\ \mathbf{q}-\mathbf{q}_h\ _{l^2(L^2)}$	Rate	$\ \nabla \cdot \mathbf{u} - \nabla \cdot \mathbf{u}_h\ _{l^2(L^2)}$	Rate	$\ \sigma-\sigma_h\ _{l^2(L^2)}$	Rate
2^{-3}	3.0913e-2	-	4.7507e-3	-	1.0811e-3	-	1.5725e-6	-	8.4123e-2	-
2^{-4}	7.7875e-3	1.98	1.1836e-3	2.00	2.7257e-3	1.98	3.9234e-7	2.00	2.1530e-2	1.96
2^{-5}	1.9509e-3	1.99	2.9566e-4	2.00	6.8487e-4	1.99	9.7956e-8	2.00	5.4427e-3	1.98
2^{-6}	4.8798e-4	1.99	7.3898e-5	2.00	1.7168e-4	1.99	2.4443e-8	2.00	1.3673e-3	1.99

Table 3 Example 1: Optimal convergence rates of the 2-field solver $WG(P_1^2, P_1^2; AC_1^2; P_1) + WG(P_1, P_1; AC_1)$ on trapezoidal meshes (slant parameter 0.35, see [47]) combined with Crank–Nicolson and $\Delta t = h$.

h	$\ \mathbf{u} - \mathbf{u}_h^{\circ}\ _{l^2(L^2)}$	Rate	$ p-p_h^{\circ} _{l^2(L^2)}$	Rate	$\ \mathbf{q} - \mathbf{q}_h\ _{l^2(L^2)}$	Rate	$\ \nabla \cdot \mathbf{u} - \nabla \cdot \mathbf{u}_h\ _{l^2(L^2)}$	Rate	$\ \sigma - \sigma_h\ _{l^2(L^2)}$	Rate
2^{-3}	3.3373e-2	-	5.1326e-3	-	1.1701e-2	-	1.6991e-6	-	9.1235e-2	-
2^{-4}	8.1258e-3	2.03	1.2353e-3	2.05	2.8470e-3	2.03	4.0944e-7	2.05	2.2512e-2	2.01
2^{-5}	1.9950e-3	2.02	3.0235e-4	2.03	7.0078e-4	2.02	1.0017e-7	2.03	5.5735e-3	2.01
2^{-6}	4.9360e-4	2.01	7.4750e-5	2.01	1.7375e-4	2.01	2.4723e-8	2.01	1.3848e-3	2.00

Example 2 (*Terzaghi's Consolidation Problem*). With known analytical solutions, the problem has been frequently tested [2,3,48]. Here we consider the domain $\Omega = (0,1) \times (-10,0)$ and the exact pressure solution along with some dimensionless quantities

$$p^*(z^*, t^*) = \sum_{i=0}^{\infty} \frac{2}{M} e^{-M^2 t^*} \sin(M z^*), \tag{48}$$

$$M = \frac{\pi(2i+1)}{2}, \quad t^* = \frac{c_v}{H^2}t, \quad z^* = \frac{z}{H},$$

with z being the distance from the drainage boundary (at the top), H = 10 the height of the domain, t the time, c_v the coefficient of consolidation, and

$$c_v = 3K \frac{(1-v)}{(1+v)} \frac{k_i}{u}$$

The problem involves the application of a surface loading to the poroelastic domain. Due to the domain's 1:10 aspect ratio, the fluid pressure near the bottom of the domain is subsequently influenced. The top surface is the drainage surface while the other 3 surfaces allow no flow. Therefore, the external loading induces compression of the solid, which leads to the drainage of fluid through the top surface.

The Terzaghi's consolidation problem assumes an external force applied at the top boundary of a fully saturated poroelastic domain, which is also the drainage boundary. All other boundaries are impermeable. See Fig. 1(a) for an illustration. Since the domain is tall enough, the fluid pressure at the bottom is supposed not to be affected in the early stage.

To test this problem, we take $\alpha=1, c_0=5.5\times 10^{-4}, \nu=0.25$, an isotropic permeability $k_i=10^{-12}$, a dynamic viscosity $\mu=10^{-6}$ (k(Pa)s) with a bulk modulus K=1000 (kPa). Then we have $c_v=0.0018$ (m²/s), Young's modulus $E=10^6$, permeability $\mathbf{K}=\kappa\mathbf{I}, \kappa=10^{-6}$. Lamé constants λ, μ are calculated accordingly. The following boundary and initial conditions are posed.

- (i) Boundary conditions for solid displacement $\mathbf{u} = [u_1, u_2]^T$: Dirichlet condition $\mathbf{u} = [0, 0]^T$ on the bottom boundary; Partial Dirichlet condition $u_1 = 0$ on the left and right boundaries; Neumann condition $\tilde{\sigma} \mathbf{n} = [0, -F]^T$, $F = 10^6$ on the top boundary.
- (ii) Boundary conditions for fluid pressure p:
 No flow (-K∇p) · n = 0 on the bottom, left, and right boundaries;
 Dirichlet condition p = 0 on the top boundary.
- (iii) Initial conditions:

Displacement: $\mathbf{u} = [0, 0]^T$;

Pressure: Known exact pressure projected to the finite element space.

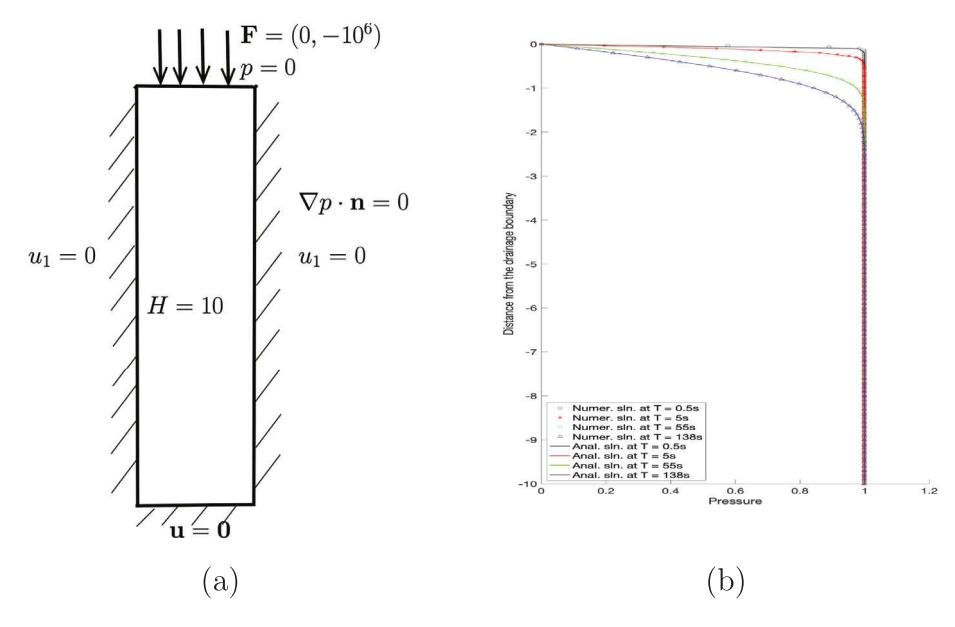


Fig. 1. Example 2: (a) An illustration of the problem; (b) Analytical (solid lines) vs. numerical (symbols) pressure along the z-axis. Black: T = 0.5 s; Red: T = 5 s; Green: T = 55 s; Blue: T = 138 s. Note that for better visualization, the height and width of the domain are not proportional.).

We test the example with the solver $WG(P_0^2, P_0^2; AC_0^2; P_0) + WG(P_0, P_0; AC_0)$ with the implicit Euler time discretization.

- When T = 0.5 s, for better approximation, we take $\Delta t = 0.1$ and spatial discretization 10×300 .
- When T = 5 s, 55 s, 138 s, we use $\Delta t = 0.1$ and spatial discretization 10×100 .

We report numerical pressures on the edges along the z-direction. Numerical and analytical pressures are presented in Fig. 1(b). Our results demonstrate nice agreement between the numerical and analytical pressures.

Example 3 (*Heterogeneous Permeability*). This example is adopted from [10] with slight modifications. We have $\Omega = (0, 1)^2$, $T = 10^{-3}$, $\lambda = 12500$, $\mu = 8333$, $\mathbf{K} = \kappa \mathbf{I}$, $c_0 = 0$, and $\alpha = 1$. The permeability is heterogeneous as shown in Fig. 2(a). In the lower-left and upperright quarters of the domain, the permeability $\kappa = 10^{-4}$, but $\kappa = 1$ elsewhere. For the displacement, an external loading (Neumann condition) is placed on the top boundary, but a homogeneous Dirichlet boundary condition is specified on other boundaries. For the pressure, the top boundary assumes the drainage (Dirichlet p = 0), while other boundaries have a no-flow (Neumann) condition.

Fig. 2(b) shows the numerical solution obtained from applying the solver $WG(P_0^2, P_0^2; AC_0^2; P_0) + WG(P_0, P_0; AC_0)$ on a rectangular mesh $(h = \frac{1}{128})$ with the implicit Euler for temporal discretization. Steep pressure fronts can be clearly observed near the internal boundaries (x = 0.5 or y = 0.5) of permeability. Fig. 2(c) presents more details of the pressure contours. No spurious pressure oscillations are spotted.

Example 3 is also solved using higher order WG(P_1^2 , P_1^2 ; AC_1^2 ; P_1) + WG(P_1 , P_1 ; AC_1) on rectangular meshes. Fig. 3(a)(c) show the results with $h = \frac{1}{64}$ and the implicit Euler with $\Delta t = \frac{T}{64 \times 64}$. Fig. 3(b)(d) show the results with $h = \frac{1}{32}$ and Crank–Nicolson with $\Delta t = \frac{T}{32}$. For comparison, both numerical pressures and contours at the final time T are plotted on the 128×128 meshes. Comparable results are observed, but the Crank–Nicolson solver uses less time steps.

6. Concluding remarks

In this paper, we have developed two sets of new finite element solvers for linear poroelasticity problems. Both sets are based on full weak Galerkin discretizations on quadrilateral meshes, which are equally flexible as triangular meshes for accommodation of complicated geometry. These solvers are developed for the primal variables, namely, solid displacement and fluid pressure. Other physical quantities such as stress, dilation, and velocity can be easily obtained via postprocessing with the weak Galerkin methodology. These solvers have optimal order spatial and temporal accuracy. Moreover, the solvers are locking-free. The robustness of these novel solvers have been demonstrated by numerical experiments on popular test cases.

Both sets of solvers developed in this paper utilize one-step temporal discretization. Each can be efficiently used as a starter solver for more sophisticated poroelasticity solvers that are based on higher order temporal discretizations.

The methodology in this paper can be applied to develop finite element solvers for 3-dim poroelasticity problems on cuboidal hexahedral meshes. Similarly, scalar- and vector-valued P-type polynomials in element interiors and on faces will be used to approximate fluid pressure and solid placement. Their discrete weak gradients will be established in broken Arbogast–Tao spaces

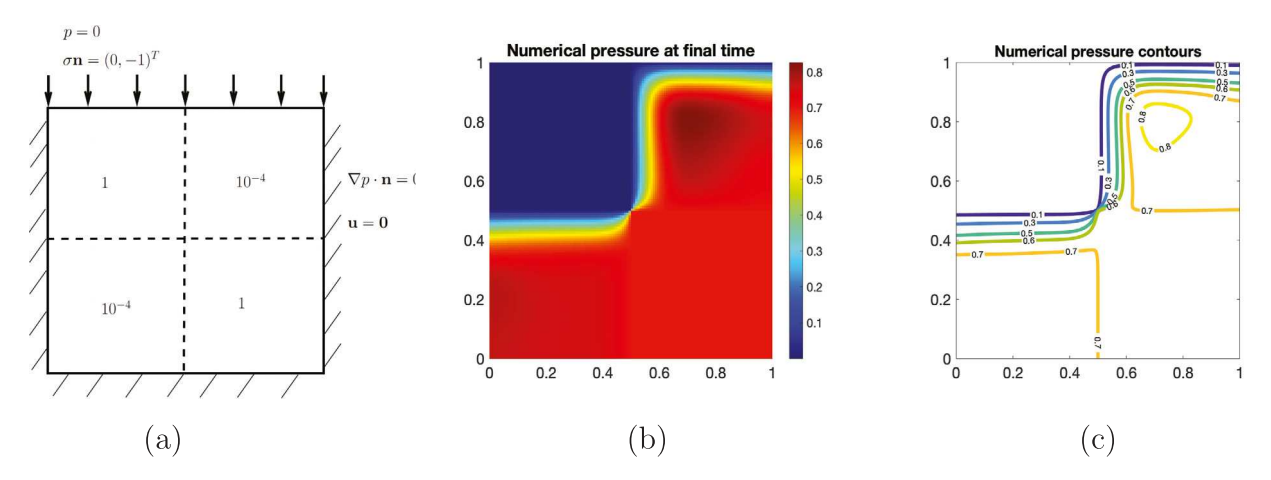


Fig. 2. Example 3: (a) Permeability profile and boundary conditions. (b) Numerical pressure at the final time $T=10^{-3}$ by Algorithm I: $WG(P_0^2,P_0^2;AC_0^2;P_0)+WG(P_0,P_0;AC_0)$ on a rectangular mesh $(h=\frac{1}{128})$ combined with the implicit Euler $(\Delta t=\frac{T}{128})$. (c) Numerical pressure contours (0.1 to 0.8).

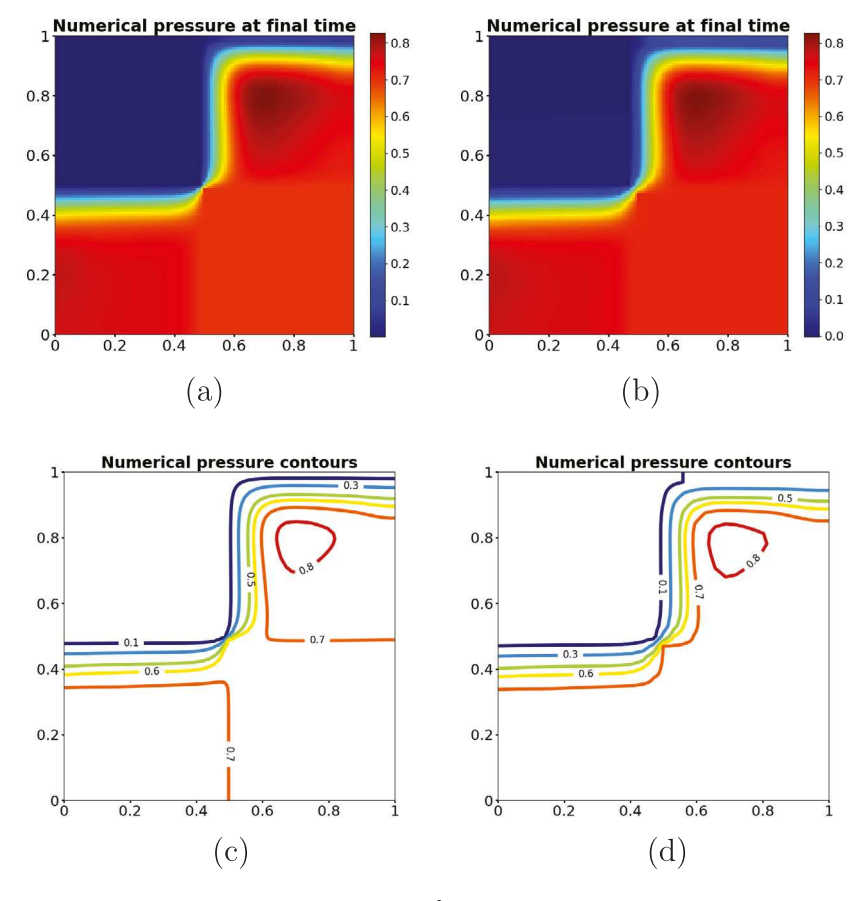


Fig. 3. Example 3: Numerical pressures and contours at the final time $T=10^{-3}$. Spatial discretization utilizes WG(P_1 , AC_1). (a)(c) Algorithm I (implicit Euler) with $h=\frac{1}{64}$, $\Delta t=\frac{T}{64\times64}$; (b)(d) Algorithm II (Crank–Nicolson) with $h=\frac{1}{32}$, $\Delta t=\frac{T}{32}$.

(of vectors or matrices) [49], for which local basis functions need to be constructed. This is under our investigation and will be reported in our future work.

These solvers can be applied to modeling and simulations of practical poroelasticity problems such as intracellular transport of viral protein and drug delivery through tissues near cancer sites. This is under our investigation and will be reported in our future work.

Data availability

Data will be made available on request.

Acknowledgments

J. Liu was partially supported by US National Science Foundation under grant DMS-2208590. S. Tavener was partially supported by US National Science Foundation under grant DMS-1720473. R. Wang was partially supported by the National Natural Science Foundation of China (grant No. 12001230, 11971198), the National Key Research and Development Program of China (grant No. 2020YFA0713602), and the Key Laboratory of Symbolic Computation and Knowledge Engineering of Ministry of Education of China housed at Jilin University.

Appendix

In the appendix, we provide complete rigorous proofs of Theorem 1, 2, and 3.

Proof of Theorem 1. For ease of presentation, we assume $\mathbf{K} = \kappa \mathbf{I}$ with $\kappa > 0$ being a constant. The proof is divided into three steps.

<u>Step (i)</u>. Take $\mathbf{v}_h = \xi_h^{(n)} - \xi_h^{(n-1)}$ and $q_h = \zeta_h^{(n)}$ in (37). Adding these terms up and applying the elementary inequality $2a(a-b) \ge a^2 - b^2$, we obtain

$$\frac{\mu}{2} \|\nabla_{w} \xi_{h}^{(n)}\|^{2} + \frac{\lambda + \mu}{2} \|\nabla_{w} \cdot \xi_{h}^{(n)}\|^{2} + \frac{c_{0}}{2} \|\xi_{h}^{\circ,(n)}\|^{2} + \Delta t \kappa \|\nabla_{w} \xi_{h}^{(n)}\|^{2}
\leq \frac{\mu}{2} \|\nabla_{w} \xi_{h}^{(n-1)}\|^{2} + \frac{\lambda + \mu}{2} \|\nabla_{w} \cdot \xi_{h}^{(n-1)}\|^{2} + \frac{c_{0}}{2} \|\xi_{h}^{\circ,(n-1)}\|^{2}
+ \sum_{E \in \mathcal{E}_{h}} (\phi(\mathbf{u}^{(n)}) + \psi(p^{(n)}), \nabla_{w} (\xi_{h}^{(n)} - \xi_{h}^{(n-1)}))_{E}
+ \Delta t \sum_{E \in \mathcal{E}_{h}} (\phi(p^{(n)}), \nabla_{w} \xi_{h}^{(n)})_{E}
+ \Delta t \sum_{E \in \mathcal{E}_{h}} (\alpha \nabla \cdot \mathbf{R}(\mathbf{u}, t_{n}) + c_{0} \mathbf{R}(p, t_{n}), \xi_{h}^{\circ,(n)})_{E}.$$
(49)

Step (ii). Applying the fact that $\|\zeta_h^{\circ,(n)}\| \le C\|\nabla_w\zeta_h^{(n)}\|$ (see [37]) and the Young's inequality, we get

$$\Delta t(\varphi(p^{(n)}), \nabla_{w}\zeta_{h}^{(n)}) \leq \frac{\Delta t \kappa}{2} \|\nabla_{w}\zeta_{h}^{(n)}\|^{2} + \frac{\Delta t}{2\kappa} \|\varphi(p^{(n)})\|^{2},$$

$$\Delta t \sum_{E \in \mathcal{E}_{h}} \alpha(\nabla \cdot \mathbf{R}(\mathbf{u}, t_{n}), \zeta_{h}^{\circ,(n)})_{E} \leq \frac{\epsilon}{2} \Delta t \|\nabla_{w}\zeta_{h}^{(n)}\|^{2}$$

$$+ \frac{\alpha^{2}C^{2}}{2\epsilon} \Delta t \|\nabla \cdot \mathbf{R}(\mathbf{u}, t_{n})\|^{2},$$

$$\Delta t \sum_{E \in \mathcal{E}_{h}} c_{0}(\mathbf{R}(p, t_{n}), \zeta_{h}^{\circ,(n)})_{E} \leq \frac{\epsilon}{2} \Delta t \|\nabla_{w}\zeta_{h}^{(n)}\|^{2} + \frac{c_{0}^{2}C^{2}}{2\epsilon} \Delta t \|\mathbf{R}(p, t_{n})\|^{2}.$$
(50)

Moreover, we have

$$\frac{\mu}{2} \|\nabla_{w} \xi_{h}^{(n)}\|^{2} + \frac{\lambda + \mu}{2} \|\nabla_{w} \cdot \xi_{h}^{(n)}\|^{2} + \frac{c_{0}}{2} \|\xi_{h}^{\circ,(n)}\|^{2}
+ \left(\frac{\kappa}{2} - \epsilon\right) \Delta t \|\nabla_{w} \xi_{h}^{(n)}\|^{2}
\leq \frac{\mu}{2} \|\nabla_{w} \xi_{h}^{(n-1)}\|^{2} + \frac{\lambda + \mu}{2} \|\nabla_{w} \cdot \xi_{h}^{(n-1)}\|^{2} + \frac{c_{0}}{2} \|\xi_{h}^{\circ,(n-1)}\|^{2}
+ \sum_{E \in \mathcal{E}_{h}} (\phi(\mathbf{u}^{(n)}) + \psi(p^{(n)}), \nabla_{w} (\xi_{h}^{(n)} - \xi_{h}^{(n-1)}))_{E}
+ \frac{\Delta t}{2\kappa} \|\phi(p^{(n)})\|^{2} + \frac{\alpha^{2} C^{2}}{2\epsilon} \Delta t \|\nabla \cdot \mathbf{R}(\mathbf{u}, t_{n})\|^{2}
+ \frac{c_{0}^{2} C^{2}}{2\epsilon} \Delta t \|\mathbf{R}(p, t_{n})\|^{2},$$
(51)

by math induction and the fact that $\xi_h^{(0)}=\mathbf{0},\, \zeta_h^{(0)}=0.$ Furthermore,

$$\frac{\mu}{2} \|\nabla_{w} \xi_{h}^{(N)}\|^{2} + \frac{\lambda + \mu}{2} \|\nabla_{w} \cdot \xi_{h}^{(N)}\|^{2} + \frac{c_{0}}{2} \|\xi_{h}^{\circ,(N)}\|^{2}
+ \sum_{n=1}^{N} \left(\frac{\kappa}{2} - \epsilon\right) \Delta t \|\nabla_{w} \xi_{h}^{(n)}\|^{2}
\leq \sum_{n=1}^{N} \sum_{E \in \mathcal{E}_{h}} (\phi(\mathbf{u}^{(n)}) + \psi(p^{(n)}), \nabla_{w} (\xi_{h}^{(n)} - \xi_{h}^{(n-1)}))_{E}
+ \sum_{n=1}^{N} \frac{\Delta t}{2\kappa} \|\varphi(p^{(n)})\|^{2} + \sum_{n=1}^{N} \frac{\alpha^{2} C^{2}}{2\epsilon} \Delta t \|\nabla \cdot \mathbf{R}(\mathbf{u}, t_{n})\|^{2}
+ \sum_{n=1}^{N} \frac{c_{0}^{2} C^{2}}{2\epsilon} \Delta t \|\mathbf{R}(p, t_{n})\|^{2}.$$
(52)

Applying the technique of summation by parts, we have

$$\sum_{n=1}^{N} a_n (b_n - b_{n-1}) = a_N b_N - a_0 b_0 - \sum_{n=1}^{N} (a_n - a_{n-1}) b_{n-1},$$

and hence

$$\frac{\mu}{2} \|\nabla_{w} \xi_{h}^{(N)}\|^{2} + \frac{\lambda + \mu}{2} \|\nabla_{w} \cdot \xi_{h}^{(N)}\|^{2} + \frac{c_{0}}{2} \|\xi_{h}^{\circ,(N)}\|^{2}
+ \sum_{n=1}^{N} \left(\frac{\kappa}{2} - \epsilon\right) \Delta t \|\nabla_{w} \xi_{h}^{(n)}\|^{2}
\leq \sum_{E \in \mathcal{E}_{h}} (\phi(\mathbf{u}^{(N)}), \nabla_{w} \xi_{h}^{(N)})_{E} + \sum_{E \in \mathcal{E}_{h}} (\psi(p^{(N)}), \nabla_{w} \xi_{h}^{(N)})_{E}
- \sum_{n=1}^{N} \sum_{E \in \mathcal{E}_{h}} (\phi(\mathbf{u}^{(n)}) - \phi(\mathbf{u}^{(n-1)}), \nabla_{w} \xi_{h}^{(n-1)})_{E}
- \sum_{n=1}^{N} \sum_{E \in \mathcal{E}_{h}} (\psi(p^{(n)}) - \psi(p^{(n-1)}), \nabla_{w} \xi_{h}^{(n-1)})_{E}
+ \sum_{n=1}^{N} \frac{\Delta t}{2\kappa} \|\varphi(p^{(n)})\|^{2} + \sum_{n=1}^{N} \frac{\alpha^{2} C^{2}}{2\epsilon} \Delta t \|\nabla \cdot \mathbf{R}(\mathbf{u}, t_{n})\|^{2}
+ \sum_{n=1}^{N} \frac{c_{0}^{2} C^{2}}{2\epsilon} \Delta t \|\mathbf{R}(p, t_{n})\|^{2}.$$
(53)

Applying the Young's inequality leads to

$$\sum_{E \in \mathcal{E}_{h}} (\phi(\mathbf{u}^{(N)}), \nabla_{w}(\xi_{h}^{(N)}))_{E} \leq \frac{\epsilon}{2} \|\nabla_{w} \xi_{h}^{(N)}\|^{2} + \frac{1}{2\epsilon} \|\phi(\mathbf{u}^{(N)})\|^{2},$$

$$\sum_{E \in \mathcal{E}_{h}} (\psi(p^{(N)}), \nabla_{w}(\xi_{h}^{(N)}))_{E} \leq \frac{\epsilon}{2} \|\nabla_{w} \xi_{h}^{(N)}\|^{2} + \frac{1}{2\epsilon} \|\psi(p^{(N)})\|^{2}.$$
(54)

Applying the fact that $\frac{\mathbf{u}^{(n)} - \mathbf{u}^{(n-1)}}{\Delta t} = \partial_t \mathbf{u}^{(n)} + \mathbf{R}(\mathbf{u}, t_n)$ yields

$$\sum_{n=1}^{N} \sum_{E \in \mathcal{E}_{h}} (\phi(\mathbf{u}^{(n)}) - \phi(\mathbf{u}^{(n-1)}), \nabla_{w}(\xi_{h}^{(n-1)}))_{E}
\leq \frac{1}{2} \sum_{n=0}^{N-1} \Delta t \|\nabla_{w} \xi_{h}^{(n)}\|^{2} + \frac{1}{2} \sum_{n=1}^{N} \Delta t \|\phi(\partial_{t} \mathbf{u}^{(n)} + \mathbf{R}(\mathbf{u}, t_{n}))\|^{2}.$$
(55)

Similarly,

$$\sum_{n=1}^{N} \sum_{E \in \mathcal{E}_{h}} (\psi(p^{(n)}) - \psi(p^{(n-1)}), \nabla_{w}(\xi_{h}^{(n-1)}))_{E}$$

$$\leq \frac{1}{2} \sum_{n=0}^{N-1} \Delta t \|\nabla_{w} \xi_{h}^{(n)}\|^{2} + \frac{1}{2} \sum_{n=1}^{N} \Delta t \|\psi(\partial_{t} p^{(n)} + \mathbf{R}(p, t_{n}))\|^{2}.$$
(56)

Combined together, these yield

$$\left(\frac{\mu}{2} - \epsilon\right) \|\nabla_{w} \xi_{h}^{(N)}\|^{2} + \frac{\lambda + \mu}{2} \|\nabla_{w} \cdot \xi_{h}^{(N)}\|^{2}
+ \frac{c_{0}}{2} \|\xi_{h}^{\circ,(N)}\|^{2} + \sum_{n=1}^{N} \left(\frac{\kappa}{2} - \epsilon\right) \Delta t \|\nabla_{w} \xi_{h}^{(n)}\|^{2}
\leq \sum_{n=0}^{N-1} \Delta t \|\nabla_{w} \xi_{h}^{(n)}\|^{2} + \frac{1}{2\epsilon} \|\phi(\mathbf{u}^{(N)})\|^{2} + \frac{1}{2\epsilon} \|\psi(p^{(N)})\|^{2}
+ \frac{1}{2} \sum_{n=1}^{N} \Delta t \|\phi(\partial_{t} \mathbf{u}^{(n)} + \mathbf{R}(\mathbf{u}, t_{n}))\|^{2} + \frac{1}{2} \sum_{n=1}^{N} \Delta t \|\psi(\partial_{t} p^{(n)} + \mathbf{R}(p, t_{n}))\|^{2}
+ \sum_{n=1}^{N} \frac{\Delta t}{2\kappa} \|\varphi(p^{(n)})\|^{2} + \sum_{n=1}^{N} \frac{\alpha^{2} C^{2}}{2\epsilon} \Delta t \|\nabla \cdot \mathbf{R}(\mathbf{u}, t_{n})\|^{2}
+ \sum_{n=1}^{N} \frac{c_{0}^{2} C^{2}}{2\epsilon} \Delta t \|\mathbf{R}(p, t_{n})\|^{2}.$$
(57)

Step (iii). Applying the commutativity (19) and the Bramble-Hilbert lemma, we obtain

$$\|\phi(\mathbf{u}^{(N)})\| \leq \mu \|\nabla_{w} \mathbf{Q}_{h} \mathbf{u}^{(N)} - \Pi_{h} \nabla \mathbf{u}^{(N)}\|$$

$$+(\lambda + \mu) \|\nabla_{w} \cdot \mathbf{Q}_{h} \mathbf{u}^{(N)} \mathbf{I} - \Pi_{h} (\nabla \cdot \mathbf{u}^{(N)} \mathbf{I})\|$$

$$= \mu \|\mathbb{Q}_{h} \nabla \mathbf{u}^{(N)} - \Pi_{h} \nabla \mathbf{u}^{(N)}\|$$

$$+(\lambda + \mu) \|(\mathbf{Q}_{h}^{\circ} \nabla \cdot \mathbf{u}^{(N)}) \mathbf{I} - \Pi_{h} (\nabla \cdot \mathbf{u}^{(N)} \mathbf{I})\|$$

$$\lesssim h^{k+1} (\mu \|\mathbf{u}^{(N)}\|_{k+2} + (\lambda + \mu) \|\nabla \cdot \mathbf{u}^{(N)}\|_{k+1})$$

$$= \mathcal{O}(h^{k+1}).$$
(58)

Similarly, we have

$$\|\psi(p^{(N)})\| \lesssim h^{k+1}\alpha \|p^{(N)}\|_{k+1} = \mathcal{O}(h^{k+1}),$$

$$\sum_{n=1}^{N} \frac{\Delta t}{2\kappa} \|\varphi(p^{(n)})\|^{2} \lesssim Th^{2(k+1)}\kappa \|\nabla p\|_{L^{\infty}(0,T;H^{k+1}(\Omega))}^{2} = \mathcal{O}(h^{2(k+1)}).$$
(59)

Moreover, there holds

$$\sum_{n=1}^{N} \Delta t \|\phi(\partial_{t} \mathbf{u}^{(n)})\|^{2} \lesssim T h^{2(k+1)} (\mu \|\partial_{t} \mathbf{u}\|_{L^{\infty}(0,T;H^{k+2}(\Omega))} + (\lambda + \mu) \|\nabla \cdot \partial_{t} \mathbf{u}\|_{L^{\infty}(0,T;H^{k+1}(\Omega))})^{2} = \mathcal{O}(h^{2(k+1)}),$$
(60)

and

$$\sum_{t=0}^{N} \Delta t \|\psi(\partial_{t} p^{(n)})\|^{2} \lesssim T h^{2(k+1)} (\alpha \|\partial_{t} p\|_{L^{\infty}(0,T;H^{k+1}(\Omega))})^{2} = \mathcal{O}(h^{2(k+1)}).$$
(61)

Applying the Cauchy-Schwarz inequality, we are led to the following estimates

$$\sum_{n=1}^{N} \Delta t \|\mathbf{R}(p, t_n)\|^2 = \sum_{n=1}^{N} \Delta t \int_{\Omega} \left(\frac{1}{\Delta t} \int_{t_{n-1}}^{t_n} (\tau - t_{n-1}) \partial_{tt} p(\tau) d\tau \right)^2 d\mathbf{x}$$

$$\leq \sum_{n=1}^{N} \frac{1}{\Delta t} \int_{\Omega} \int_{t_{n-1}}^{t_n} (\tau - t_{n-1})^2 d\tau \int_{t_{n-1}}^{t_n} \partial_{tt} p(\tau)^2 d\tau d\mathbf{x}$$

$$\lesssim (\Delta t)^2 \int_{0}^{T} \|\partial_{tt} p\|^2 d\tau = \mathcal{O}(\Delta t^2). \tag{62}$$

Similarly,

$$\sum_{n=1}^{N} \Delta t \|\phi(\mathbf{R}(\mathbf{u}, t_n))\|^2$$

$$\lesssim \Delta t^2 h^{2(k+1)} \int_0^T (\mu \|\partial_{tt} \mathbf{u}\|_{k+2} + (\lambda + \mu) \|\nabla \cdot \partial_{tt} \mathbf{u}\|_{k+1})^2 d\tau$$

$$= \mathcal{O}((\Delta t)^2 h^{2(k+1)}),$$
(63)

R. Wang et al.

and

$$\sum_{n=1}^{N} \Delta t \| \boldsymbol{\psi}(\mathbf{R}(p, t_n)) \|^2 \lesssim (\Delta t)^2 h^{2(k+1)} \int_0^T (\alpha \| \partial_{tt} \boldsymbol{p} \|_{k+1})^2 d\tau
= \mathcal{O}((\Delta t)^2 h^{2(k+1)}),$$

$$\sum_{n=1}^{N} \Delta t \| \nabla \cdot \mathbf{R}(\mathbf{u}, t_n) \|^2 \lesssim \Delta t^2 \int_0^T \| \partial_{tt} \nabla \cdot \mathbf{u} \|^2 d\tau = \mathcal{O}((\Delta t)^2).$$
(64)

Therefore, there holds

$$\left(\frac{\mu}{2} - \epsilon\right) \|\nabla_{w} \xi_{h}^{(N)}\|^{2} + \frac{\lambda + \mu}{2} \|\nabla_{w} \cdot \xi_{h}^{(N)}\|^{2}
+ \frac{c_{0}}{2} \|\xi_{h}^{\circ,(N)}\|^{2} + \sum_{n=1}^{N} \left(\frac{\kappa}{2} - \epsilon\right) \Delta t \|\nabla_{w} \xi_{h}^{(n)}\|^{2}
\leq \Delta t \sum_{n=0}^{N-1} \|\nabla_{w} (\xi_{h}^{(n)})\|^{2} + \mathcal{O}(h^{2(k+1)} + (\Delta t)^{2}).$$
(65)

Finally, the discrete Gronwall inequality leads to

$$\max_{1 \le n \le N} \left\{ \left(\frac{\mu}{2} - \epsilon \right) \| \nabla_{w} \xi_{h}^{(n)} \|^{2} + \frac{\lambda + \mu}{2} \| \nabla_{w} \cdot \xi_{h}^{(n)} \|^{2} + \frac{c_{0}}{2} \| \xi_{h}^{\circ,(n)} \|^{2} \right\} \\
+ \sum_{n=1}^{N} \left(\frac{\kappa}{2} - \epsilon \right) \Delta t \| \nabla_{w} \xi_{h}^{(n)} \|^{2} \\
\le \mathcal{O}(h^{2(k+1)} + (\Delta t)^{2}), \tag{66}$$

which completes the proof of Theorem 1. \square

Proof of Theorem 2. The proof is divided into three steps.

Step (i). Take $\mathbf{v}_h = \xi_h^{(n)} - \xi_h^{(n-1)}$ and $q_h = \overline{\xi}_h^{n-\frac{1}{2}}$ in (42). Adding these them up and applying the elementary identity $(a+b)(a-b) = a^2 - b^2$, we obtain

$$\frac{\mu}{2} \|\nabla_{w} \xi_{h}^{(n)}\|^{2} + \frac{\lambda + \mu}{2} \|\nabla_{w} \cdot \xi_{h}^{(n)}\|^{2} + \frac{c_{0}}{2} \|\xi_{h}^{\circ,(n)}\|^{2} + \Delta t \,\kappa \|\nabla_{w} \bar{\xi}_{h}^{n-\frac{1}{2}}\|^{2} \\
\leq \frac{\mu}{2} \|\nabla_{w} \xi_{h}^{(n-1)}\|^{2} + \frac{\lambda + \mu}{2} \|\nabla_{w} \cdot \xi_{h}^{(n-1)}\|^{2} + \frac{c_{0}}{2} \|\xi_{h}^{\circ,(n-1)}\|^{2} \\
+ \sum_{E \in \mathcal{E}_{h}} (\phi(\bar{\mathbf{u}}^{n-\frac{1}{2}}) + \psi(\bar{p}^{n-\frac{1}{2}}), \nabla_{w} (\xi_{h}^{(n)} - \xi_{h}^{(n-1)}))_{E} \\
+ \sum_{E \in \mathcal{E}_{h}} \Delta t(\phi(\bar{p}^{n-\frac{1}{2}}), \nabla_{w} \bar{\xi}_{h}^{n-\frac{1}{2}})_{E} \\
+ \Delta t \sum_{E \in \mathcal{E}_{h}} (\alpha \nabla \cdot \tilde{\mathbf{R}}(\mathbf{u}, t_{n}) + c_{0} \tilde{\mathbf{R}}(p, t_{n}), \bar{\xi}_{h}^{\circ, n-\frac{1}{2}})_{E}. \tag{67}$$

Step (ii). Applying the techniques in Theorem 1 proof Step (ii), we obtain

$$\left(\frac{\mu}{2} - \epsilon\right) \|\nabla_{w} \xi_{h}^{(N)}\|^{2} + \frac{\lambda + \mu}{2} \|\nabla_{w} \cdot \xi_{h}^{(N)}\|^{2} + \frac{c_{0}}{2} \|\xi_{h}^{\circ(N)}\|^{2} + \sum_{n=1}^{N} \left(\frac{\kappa}{2} - \epsilon\right) \Delta t \|\nabla_{w} \xi_{h}^{(N)}\|^{2} \right) \\
\leq \Delta t \sum_{n=0}^{N-1} \|\nabla_{w} \xi_{h}^{(n)}\|^{2} + \frac{1}{2\epsilon} \|\phi(\bar{\mathbf{u}}^{N-\frac{1}{2}})\|^{2} + \frac{1}{2\epsilon} \|\psi(\bar{p}^{N-\frac{1}{2}})\|^{2} \\
+ \frac{1}{2} \Delta t \sum_{n=1}^{N} \|\phi(\partial_{t} \bar{\mathbf{u}}^{n-\frac{1}{2}} + \tilde{\mathbf{R}}(\mathbf{u}, t_{n}))\|^{2} \\
+ \frac{1}{2} \Delta t \sum_{n=1}^{N} \|\psi(\partial_{t} \bar{p}^{n-\frac{1}{2}} + \tilde{\mathbf{R}}(p, t_{n}))\|^{2} \\
+ \sum_{n=1}^{N} \frac{\Delta t}{2\kappa} \|\varphi(\bar{p}^{n-\frac{1}{2}})\|^{2} + \sum_{n=1}^{N} \frac{\alpha^{2} C^{2}}{2\epsilon} \Delta t \|\nabla \cdot \tilde{\mathbf{R}}(\mathbf{u}, t_{n})\|^{2} \\
+ \sum_{n=1}^{N} \frac{c_{0}^{2} C^{2}}{2\epsilon} \Delta t \|\tilde{\mathbf{R}}(p, t_{n})\|^{2}. \tag{68}$$

Step (iii). Since

$$\widetilde{\mathbf{R}}(\mathbf{u},t_n) = \frac{\mathbf{u}^{(n)} - \mathbf{u}^{(n-1)}}{\Delta t} - \partial_t \overline{\mathbf{u}}^{n-\frac{1}{2}} = \mathcal{O}(\Delta t^2),$$

$$\widetilde{\mathbf{R}}(p,t_n) = \frac{p^{(n)} - p^{(n-1)}}{\Delta t} - \partial_t \overline{p}^{n-\frac{1}{2}} = \mathcal{O}(\Delta t^2),$$

we have

$$\max_{1 \le n \le N} \left\{ \left(\frac{\mu}{2} - \epsilon \right) \| \nabla_{w} \xi_{h}^{(n)} \|^{2} + \frac{\lambda + \mu}{2} \| \nabla_{w} \cdot \xi_{h}^{(n)} \|^{2} + \frac{c_{0}}{2} \| \xi_{h}^{\circ,(n)} \|^{2} \right\} \\
+ \sum_{n=1}^{N} \left(\frac{\kappa}{2} - \epsilon \right) \Delta t \| \nabla_{w} \tilde{\xi}_{h}^{n - \frac{1}{2}} \|^{2} \\
\le \mathcal{O}(h^{4} + \Delta t^{4}).$$
(69)

which implies the conclusion of Theorem 2. \square

Proof of Theorem 3. Applying the same techniques as in the proof of Theorem 1, we obtain

$$\begin{split} & \Big(\frac{\mu}{2} - \epsilon\Big) \|\nabla_w \xi_h^{(N)}\|^2 \leq \sum_{n=0}^{N-1} \Delta t \|\nabla_w \xi_h^{(n)}\|^2 + \frac{1}{2\epsilon} \|\phi(\mathbf{u}^{(N)})\|^2 \\ & + \frac{1}{2\epsilon} \|\psi(p^{(N)})\|^2 + \frac{1}{2} \sum_{n=1}^{N} \Delta t \|\phi(\partial_t \mathbf{u}^{(n)} + \mathbf{R}(\mathbf{u}, t_n))\|^2 \\ & + \frac{1}{2} \sum_{n=1}^{N} \Delta t \|\psi(\partial_t p^{(n)} + \mathbf{R}(p, t_n))\|^2 + \sum_{n=1}^{N} \frac{\Delta t}{2\epsilon} \|\varphi(p^{(n)})\|^2 \\ & + \sum_{n=1}^{N} \frac{\alpha^2 C^2}{2\epsilon} \Delta t \|\nabla \cdot \mathbf{R}(\mathbf{u}, t_n)\|^2 + \sum_{n=1}^{N} \frac{c_0^2 C^2}{2\epsilon} \Delta t \|\mathbf{R}(p, t_n)\|^2. \end{split}$$

For k = 0, under the regularity assumption

$$\mu \|\mathbf{u}\|_2 + \lambda \|\nabla \cdot \mathbf{u}\|_1 \le C \|\mathbf{f}\|_0,$$

we have, by applying the commuting identities,

$$\begin{split} \|\phi(\mathbf{u}^{(N)})\| &= \left\| \mu(\nabla_w(\mathbf{Q}_h\mathbf{u}^{(n)}) - \Pi_h(\nabla\mathbf{u}^{(n)})) \right. \\ &+ (\lambda + \mu)(\nabla_w \cdot (\mathbf{Q}_h\mathbf{u}^{(n)})\mathbf{I} - \Pi_h((\nabla \cdot \mathbf{u}^{(n)})\mathbf{I})) \right\| \\ &\leq \mu \|\mathbb{Q}_h(\nabla\mathbf{u}^{(N)}) - \Pi_h(\nabla\mathbf{u}^{(N)})\| \\ &+ (\lambda + \mu)\|(Q_h^\circ(\nabla \cdot \mathbf{u}^{(N)}))\mathbf{I} - \Pi_h((\nabla \cdot \mathbf{u}^{(N)})\mathbf{I})\| \\ &\leq Ch\left(\mu \|\mathbf{u}^{(N)}\|_2 + (\lambda + \mu)\|\nabla \cdot \mathbf{u}^{(N)}\|_1\right) \\ &\leq Ch\left\|\mathbf{f}^{(N)}\|. \end{split}$$

Similarly, we obtain, with the constant C > 0 being independent of λ and h,

$$\sum_{n=1}^{N} \Delta t \|\phi(\partial_t \mathbf{u}^{(n)})\|^2 \le Ch^2 \|\partial_t \mathbf{f}\|_{L^{\infty}(0,T;L^2(\Omega))}^2,$$

$$\sum_{n=1}^{N} \Delta t \|\phi(\mathbf{R}(\mathbf{u},t_n))\|^2 \le C(\Delta t)^2 h^2 \int_0^T \|\partial_{tt} \mathbf{f}\|^2 d\tau.$$

The same techniques in Theorem 1 proof yield the following six estimates

$$\begin{split} &\|\psi(p^{(N)})\| \leq Ch\|p^{(N)}\|_1, \\ &\sum_{n=1}^N \frac{\Delta t}{2\kappa} \|\varphi(p^{(n)})\|^2 \leq Ch^2 \|\nabla p\|_{L^\infty(0,T;H^1(\Omega))}^2, \\ &\sum_{n=1}^N \Delta t \|\psi(\partial_t p^{(n)})\|^2 \leq Ch^2 \|\partial_t p\|_{L^\infty(0,T;H^1(\Omega))}^2, \\ &\sum_{n=1}^N \Delta t \|\mathbf{R}(p,t_n)\|^2 \leq C(\Delta t)^2 \int_0^T \|\partial_{tt} p\|^2 d\tau, \\ &\sum_{n=1}^N \Delta t \|\psi(\mathbf{R}(p,t_n))\|^2 \leq C(\Delta t)^2 h^2 \int_0^T (\alpha \|\partial_{tt} p\|_1)^2 d\tau, \\ &\sum_{n=1}^N \Delta t \|\nabla \cdot \mathbf{R}(\mathbf{u},t_n)\|^2 \leq C\Delta t^2 \int_0^T \|\partial_{tt} \nabla \cdot \mathbf{u}\|^2 d\tau. \end{split}$$

Combined together, they imply

$$\left(\frac{\mu}{2} - \epsilon\right) \|\nabla_w \xi_h^{(N)}\|^2 \le \Delta t \sum_{n=0}^{N-1} \|\nabla_w (\xi_h^{(n)})\|^2 + C\left(h^2 + (\Delta t)^2\right).$$

The discrete Gronwall inequality gives

$$\max_{1 \le n \le N} \|\nabla_w \xi_h^{(n)}\| \le C(h + \Delta t),$$

where the positive constant C is independent of λ and h. The second inequality in (45) follows from the estimate shown above, the properties of the projection operators, and a triangle inequality. This completes proof of Theorem 3 for the case k = 0.

As for $k \ge 1$, we need a stronger regularity assumption as shown below.

$$\mu \|\mathbf{u}\|_{k+2} + \lambda \|\nabla \cdot \mathbf{u}\|_{k+1} \le C \|\mathbf{f}\|_{k}.$$

Then we have

$$\begin{split} \|\phi(\mathbf{u}^{(N)})\| &\leq \mu \|\mathbb{Q}_h \nabla \mathbf{u}^{(N)} - \boldsymbol{\Pi}_h \nabla \mathbf{u}^{(N)} \| \\ &+ (\lambda + \mu) \|(\boldsymbol{Q}_h^{\circ} \nabla \cdot \mathbf{u}^{(N)}) \mathbf{I} - \boldsymbol{\Pi}_h (\nabla \cdot \mathbf{u}^{(N)} \mathbf{I}) \| \\ &\leq C h^{k+1} (\mu \|\mathbf{u}^{(N)}\|_{k+2} + (\lambda + \mu) \|\nabla \cdot \mathbf{u}^{(N)}\|_{k+1}) \\ &\leq C h^{k+1} \|\mathbf{f}^{(N)}\|_{k}. \end{split}$$

Similarly,

$$\begin{split} & \sum_{n=1}^{N} \Delta t \|\phi(\partial_{t}\mathbf{u}^{(n)})\|^{2} \leq C h^{2(k+1)} \|\partial_{t}\mathbf{f}\|_{L^{\infty}(0,T;H^{k}(\Omega))}^{2}, \\ & \sum_{n=1}^{N} \Delta t \|\phi(\mathbf{R}(\mathbf{u},t_{n}))\|^{2} \leq C (\Delta t)^{2} h^{2(k+1)} \int_{0}^{T} \|\partial_{tt}\mathbf{f}\|_{k}^{2} d\tau, \end{split}$$

where the constant C > 0 is independent of λ and h. Once again, the techniques for proving Theorem 1 produce

$$\begin{split} &\|\psi(p^{(N)})\| \leq Ch^{k+1}\|p^{(N)}\|_{k+1}, \\ &\sum_{n=1}^{N} \frac{\Delta t}{2\kappa} \|\varphi(p^{(n)})\|^{2} \leq Ch^{2(k+1)}\|\nabla p\|_{L^{\infty}(0,T;\,H^{k+1}(\Omega))}^{2}, \\ &\sum_{n=1}^{N} \Delta t \|\psi(\partial_{t}p^{(n)})\|^{2} \leq Ch^{2(k+1)}\|\partial_{t}p\|_{L^{\infty}(0,T;H^{k+1}(\Omega))}^{2}, \\ &\sum_{n=1}^{N} \Delta t \|\mathbf{R}(p,t_{n})\|^{2} \leq C(\Delta t)^{2} \int_{0}^{T} \|\partial_{tt}p\|^{2} d\tau, \\ &\sum_{n=1}^{N} \Delta t \|\psi(\mathbf{R}(p,t_{n}))\|^{2} \leq C(\Delta t)^{2} h^{2(k+1)} \int_{0}^{T} (\|\partial_{tt}p\|_{k+1})^{2} d\tau, \\ &\sum_{n=1}^{N} \Delta t \|\nabla \cdot \mathbf{R}(\mathbf{u},t_{n})\|^{2} \leq C\Delta t^{2} \int_{0}^{T} \|\partial_{tt}\nabla \cdot \mathbf{u}\|^{2} d\tau. \end{split}$$

Together with the discrete Gronwall inequality, they imply

$$\max_{1 \le n \le N} \| \mathbf{Q}_h \mathbf{u}^{(n)} - \mathbf{u}_h^{(n)} \| \le C \left(h^{k+1} + \Delta t \right),$$

where the constant C > 0 is independent of λ and h. The previous comment applies also to the second inequality in (47).

References

- [1] S. Barbeiro, M. Wheeler, A priori error estimates for the numerical solution of a coupled geomechanics and reservoir flow model with stress-dependent permeability, Comput. Geosci. 14 (2010) 755–768.
- [2] F.J. Carrillo, I.C. Bourg, Modeling multiphas flow within and around deformable porous materials: a Darcy-Brinkman-Biot approach, Water Resour. Res. (2021).
- [3] J. Choo, S. Lee, Enriched Galerkin finite elements for coupled poromechanics with local mass conservation, Comput. Methods Appl. Mech. Engrg. 341 (2018) 311–332.
- [4] J. Coulet, I. Faille, V. Girault, N. Guy, F. Nataf, A fully coupled scheme using virtual element method and finite volume for poroelasticity, Comput. Geosci. 24 (2020) 381–403.
- [5] M.R. Islam., J. Virag, M.L. Oyen, Micromechanical poroelastic and viscoelastic properties of ex-vivo soft tissues, J. Biomech. (2020).
- [6] R. Oftadeh, B.K. Connizzo, H.T. Nia, C. Ortiz, Biological connective tissues exhibit viscoelstic and poroelastic behavior at different frequency regimes: Application to tendon and skin biophysics, Acta Biomater. (2018).
- [7] E. Moeendarbary, L. Valon, M. Fritzsche, A.R. Harris, D.A. Moulding, A.J. Thrasher, E. Stride, L. Mahadevan, G.T. Charras, The cytoplasm of living cells behaves as a poroelastic material, Nature Mater. 12 (3) (2013) 253–261.
- [8] L. Berger, R. Bordas, D. Kay, S. Tavener, Stabilized lowest-order finite element approximation for linear three-field poroelasticity, SIAM J. Sci. Comput. 37 (2015) A2222–A2245.
- [9] X. Feng, Z. Ge, Y. Li, Analysis of a multiphysics finite element method for a poroelasticity model, IMA J. Numer. Anal. 38 (2018) 330-359.
- [10] X. Hu, C. Rodrigo, F. Gaspar, L. Zikatanov, A nonconforming finite element method for the Biot's consolidation model in poroelasticity, J. Comput. Appl. Math. 310 (2017) 143–154.
- [11] C. Niu, H. Rui, X. Hu, A stabilized hybrid mixed finite element method for poroelasticity, Comput. Geosci. 25 (2021) 757-774.
- [12] R. Oyarzua, R. Ruiz-Baier, Locking-free finite element methods for poroelasticity, SIAM J. Numer. Anal. 54 (2016) 2951-2973.
- [13] S.-Y. Yi, A study of two modes of locking in poroelasticity, SIAM J. Numer. Anal. 55 (2017) 1915–1936.
- [14] S.-Y. Yi, Convergence analysis of a new mixed finite element method for Biot's consolidation model, Numer. Meth. PDEs 30 (2014) 1189-1210.
- [15] W.M. Boon, A. Fumagalli, A. Scotti, Mixed and multipoint finite element methods for rotation-based poroelasticity, SIAM J. Numer. Anal. 61 (5) (2023) 2485–2508.
- [16] F. Brezzi, M. Fortin, Mixed and Hybrid Finite Element Methods, Springer, 1991.
- [17] I. Ambartsumyan, E. Khattatov, I. Yotov, A coupled multipoint stress multipoint flux mixed finite element method for the Biot system of poroelasticity, Comput. Methods Appl. Mech. Engrg. 372 (2020) 113407.
- [18] R. Bürger, S. Kumar, D. Mora, R. Ruiz-Baier, N. Verma, Virtual element methods for the three-field formulation of time-dependent linear poroelasticity, Adv. Comput. Math. 47 (2021) Article# 2.
- [19] J. Guo, M. Feng, A robust and mass conservative virtual element method for linear three-field poroelasticity, J. Sci. Comput. 92 (2022) 95.
- [20] S. Sun, J. Liu, A locally conservative finite element method based on piecewise constant enrichment of the continuous Galerkin method, SIAM J. Sci. Comput. 31 (2009) 2528–2548.
- [21] T. Kadeethum, H. Nick, S. Lee, F. Ballarin, Enriched Galerkin discretization for modeling poroelasticity and permeability alteration in heterogeneous porous media, J. Comput. Phys. 427 (2021) 110030.
- [22] S. Lee, S.-Y. Yi, Locking-free and locally-conservative enriched Galerkin method for poroelasticity, J. Sci. Comput. 94 (2023) 26.
- [23] J. Wang, X. Ye, A weak Galerkin finite element method for second order elliptic problems, J. Comput. Appl. Math. 241 (2013) 103-115.
- [24] J. Liu, S. Tavener, Z. Wang, Lowest-order weak Galerkin finite element method for Darcy flow on convex polygonal meshes, SIAM J. Sci. Comput. 40 (2018) B1229–B1252.
- [25] Z. Wang, R. Wang, J. Liu, Robust weak Galerkin finite element solvers for Stokes flow based on a lifting operator, Comput. Math. Appl. 125 (2022) 90–100.
- [26] G. Chen, X. Xie, A robust weak Galerkin finite element method for linear elasticity with strong symmetric stresses, Comput. Methods Appl. Math. 16 (3) (2016) 389–408.
- [27] C. Wang, J. Wang, R. Wang, R. Zhang, A locking-free weak Galerkin finite element method for elasticity problems in the primal formulation, J. Comput. Appl. Math. 307 (2016) 346–366.
- [28] L. Mu, J. Wang, X. Ye, S. Zhang, A weak Galerkin finite element method for the Maxwell equations, J. Sci. Comput. 65 (1) (2015) 363-386.
- [29] J. Wang, O. Zhai, R. Zhang, S. Zhang, A weak Galerkin finite element scheme for the Cahn-Hilliard equation, Math. Comp. 88 (2019) 211-235.
- [30] Z. Dong, A. Ern, Hybrid high-order and weak Galerkin methods for the biharmonic problem, SIAM J. Numer. Anal. 60 (5) (2022) 2626-2656.
- [31] W. Huang, Y. Wang, Discrete maximum principle for the weak Galerkin method for anisotropic diffusion problems, Commun. Comput. Phys. 18 (1) (2015) 65–90.
- [32] R. Li, Y. Gao, J. Li, Z. Chen, A weak Galerkin finite element method for a coupled Stokes-Darcy problem on general meshes, J. Comput. Appl. Math. 334 (2018) 111–127.
- [33] F. Gao, X. Wang, A modified weak Galerkin finite element method for a class of parabolic problems, J. Comput. Appl. Math. 271 (2014) 1-19.
- [34] S. Gu, S. Chai, C. Zhou, J. Zhou, Weak Galerkin finite element method for linear poroelasticity problems, Appl. Numer. Math. 190 (2023) 200-219.
- [35] X. Hu, L. Mu, X. Ye, Weak Galerkin method for the Biot's consolidation model, Comput. Math. Appl. 75 (2018) 2017-2030.
- [36] M. Sun, H. Rui, A coupling of weak Galerkin and mixed finite element methods for poroelasticity, Comput. Math. Appl. 73 (5) (2017) 804-823.
- [37] Z. Wang, S. Tavener, J. Liu, Analysis of a 2-field finite element solver for poroelasticity on quadrilateral meshes, J. Comput. Appl. Math. 393 (2021) Paper No. 113539, 21.
- [38] Z. Wang, J. Liu, deal.II implementation of a two-field finite element solver for poroelasticity, Lect. Notes Comput. Sci. 12143 (2020) 88-101.
- [39] J. Liu, S. Tavener, Z. Wang, Penalty-free any-order weak Galerkin FEMs for elliptic problems on quadrilateral meshes, J. Sci. Comput. 83 (2020) 47.
- [40] R. Wang, Z. Wang, J. Liu, Penalty-free any-order weak Galerkin FEMs for linear elasticity on quadrilateral meshes, J. Sci. Comput. 95 (2023) 20.
- [41] T. Arbogast, M.R. Correa, Two families of H(div) mixed finite elements on quadrilaterals of minimal dimension, SIAM J. Numer. Anal. 54 (2016) 3332–3356.
- [42] S.-Y. Yi, A lowest-order weak Galerkin method for linear elasticity, J. Comput. Appl. Math. 350 (2019) 286–298.
- [43] S.C. Brenner, L.R. Scott, The Mathematical Theory of Finite Element Methods, third ed., in: Texts in Applied Mathematics, vol. 15, Springer-Verlag, New York, 2008.
- [44] S.C. Brenner, L.-Y. Sung, Linear finite element methods for planar linear elasticity, Math. Comp. 59 (200) (1992) 321-338.

- [45] D.A. Di Pietro, A. Ern, A hybrid high-order locking-free method for linear elasticity on general meshes, Comput. Methods Appl. Mech. Engrg. 283 (2015)
- [46] J.J. Lee, E. Piersanti, K.-A. Mardal, M.E. Rognes, A mixed finite element method for nearly incompressible multiple-network poroelasticity, SIAM J. Sci. Comput. 41 (2) (2019).
- [47] G. Harper, J. Liu, S. Tavener, T. Wildey, Coupling Arbogast-Correa and Bernardi-Raugel elements to resolve coupled Stokes-Darcy flow problems, Comput. Methods Appl. Mech. Engrg. 373 (2021) 113469.
- [48] P. Phillips, M. Wheeler, A coupling of mixed with continuous Galerkin finite element methods for poroelasticity II: the-discrete-in-time case, Comput. Geosci. 11 (2007) 145–158.
- [49] T. Arbogast, Z. Tao, Construction of H(div)-conforming mixed finite elements on cuboidal hexahedra, Numer. Math. 142 (2019) 1-32.